Distribution Agreement

In presenting this thesis as a partial fulfillment of the requirements for a degree from Emory University, I hereby grant to Emory University and its agents the non-exclusive license to archive, make accessible, and display my thesis in whole or in part in all forms of media, now or hereafter now, including display on the World Wide Web. I understand that I may select some access restrictions as part of the online submission of this thesis. I retain all ownership rights to the copyright of the thesis. I also retain the right to use in future works (such as articles or books) all or part of this thesis.

Jiabao Zhong April 13, 2020

Growth inhibitory activity of *Rosa × damascena* flower extract on *Acinetobacter baumannii*

by

Jiabao Zhong

Dr. Cassandra Quave
Adviser

Biology

Dr. Cassandra Quave

Adviser

Dr. Kathleen Campbell

Committee Member

Dr. Dennis Liotta

Committee Member

Dr. Philip Rather

Committee Member

2020

Growth inhibitory activity of *Rosa × damascena* flower extract on *Acinetobacter baumannii*

By

Jiabao Zhong

Dr. Cassandra Quave

Adviser

An abstract of
a thesis submitted to the Faculty of Emory College of Arts and Sciences
of Emory University in partial fulfillment
of the requirements of the degree of
Bachelor of Science with Honors

Biology

2020

Abstract

Growth inhibitory activity of *Rosa × damascena* flower extract on *Acinetobacter baumannii*
By Jiabao Zhong

The emergence of *Acinetobacter baumannii*, a common nosocomial, opportunistic pathogen, has caused more and more infection cases around the world. The virulence of the species – tolerance for desiccation and disinfection, motility and biofilm formation – allows it to persist and spread in healthcare settings. Due to the high mortality rate and high multidrug-resistance rate, effective treatments against the pathogen are becoming limited, while the resistance genes are rapidly spread via horizontal-gene transfer between strains of *A. baumannii*. The most commonly used antibiotics against *A. baumannii* infection is carbapenem, and the last-line treatment is colistin, but strains resistant to the two antibiotics are reported around the world. The need for novel treatment is urgent and one of the promising novel treatments is chemical compounds extracted from medicinal plants.

The flower of the Damask rose, *Rosa × damascena*, has a long history of medicinal use in Lebanon, besides its various commercial use. It is commonly used to relieve gastrointestinal problems, cough and dermatitis by Lebanese, and is believed to function as cardiotonic, antirheumatic, antioxidant and antimicrobial. The essential oil of the flower is also documented to be a relaxant that heals depression, stress, anxiety and migraine. Previous research had demonstrated certain antimicrobial effect of *R. damascena* extract.

Through bioassay-guide fractionation, extraction of the *Rosa × damascena* flower was fractionated and determined to have growth inhibitory activity against *Acinetobacter baumannii* strains ATCC 17978 and AB5075. The growth inhibitory effect was determined by broth microdilution MIC assay, and the most potent fractions, 1921D-F7~9, were confirmed with TLC-agar overlay bioautography assay of inhibiting growth of AB5075. Cytotoxicity test show that the potent extracts have low toxicity to human skin cells. Therefore, further separation of the potent extracts 1921D-F7~9 of *R. damascena* flower is a promising direction for treatment against multidrug-resistant *A. baumannii*.

Growth inhibitory activity of *Rosa × damascena* flower extract on *Acinetobacter baumannii*

By

Jiabao Zhong

Dr. Cassandra Quave

Adviser

A thesis submitted to the Faculty of Emory College of Arts and Sciences
of Emory University in partial fulfillment
of the requirements of the degree of
Bachelor of Science with Honors

Biology

2020

Acknowledgements

Dr. Quave – thank you so much for giving me the chance to work in the lab and on this project

Dr. Lyles – thank you for being patient and helpful every time I have a question

Dr. Roula Abdel-Massih – thank you for bringing this beautiful plant to the Quave lab and started this project

Micah – thank you for your help with the microbiology part of the project

Danielle – thank you for helping me with the cytotoxicity test

Michelle – thank you for always willing to help me and giving me encouragement

Dr. Quave, Dr. Campbell, Dr. Liotta and Dr. Rather – thank you all for being my committee members, giving me helpful suggestions and being understanding when I have to change the schedule twice

Table of Contents

Chapter 1: Introduction **1**

Acinetobacter baumannii: emerging infection, virulence, antimicrobial resistance

Rosa × damascena mill L.: traditional use, chemical profile, pharmacological properties

Research question and project aims

Chapter 2: Materials and Methods **11**

Overview of Bioassay-guided fractionation

Plant collection and processing

Plant Maceration

Fractionation of plant extracts

Analysis of plant extracts

Bioactivity assays

Chapter 3: Results **23**

Overall fractionation scheme

Extracts 1921 and 1921B~E

Extracts 1921D and 1921D-Fs

Extracts 1921D-F7~9

Chapter 4: Discussion **39**

Overall fractionation scheme

Chemical Properties of *Rosa × damascena* Potent Extracts

Biological Activity of *Rosa × damascena* Potent Extracts

Conclusion

Future directions

List of Tables and Figures

Figure 1.1. The flower of *Rosa × damascena* mill L., the Damask rose 5

Figure 2.1. The overall scheme of bioassay-guided fractionation of *Rosa × damascena* flower extract 11

Table 2.1. Mobile phase tested for reverse-phase TLC of extracts 1921D-F7~9 18

Table 2.2. ESKAPE pathogen strains used in broth microdilution MIC assay of extracts 1921 and 1921B~E 18

Figure 3.1. Parent-child tree of the isolation scheme of *Rosa × damascena* flower extract 23

Figure 3.2. Analytical HPLC chromatogram of extract 1921 obtained under 280 nm with. %B gradient overlaid 24

Figure 3.3. Analytical HPLC chromatogram of extract 1921B obtained under 280 nm with %B gradient overlaid 24

Figure 3.4. Analytical HPLC chromatogram of extract 1921C obtained under 280 nm with %B gradient overlaid 25

Figure 3.5. Analytical HPLC chromatogram of extract 1921D obtained under 280 nm with %B gradient overlaid 25

Figure 3.6. Analytical HPLC chromatogram of extract 1921E obtained under 280 nm with %B gradient overlaid 26

Figure 3.7. Percent growth inhibition of *Rosa × damascena* crude and partition extracts against ESKAPE pathogens 27

Table 3.1. IC50 of 1921 and 1921B~E against ESKAPE Pathogens (µg/mL) 28

Figure 3.8. Flash chromatogram of 1921D obtained under 280 nm with %B gradient overlaid 29

Figure 3.9. Normal-phase TLC of 1921D flash solutions 30

Figure 3.10. Normal-phase TLC of 1921D and 1921D-F7~9 31

Figure 3.11. Analytical HPLC chromatogram of extracts 1921D-F7 and 1921D obtained under 254 nm with %B gradient overlaid 31

Figure 3.12. Analytical HPLC chromatogram of extracts 1921D-F8 and 1921D obtained under 254 nm with %B gradient overlaid 32

Figure 3.13. Analytical HPLC chromatogram of extracts 1921D-F9 and 1921D obtained under 254 nm with %B gradient overlaid 32

Figure 3.14. Analytical HPLC chromatogram of extracts 1921D-F7~9 obtained under 254 nm with %B gradient overlaid 33

Figure 3.15. Percent growth inhibition of *Rosa × damascena* flash extracts against *Acinetobacter baumannii* 34

Table 3.2. IC50 of 1921D-F1~11 Against *Acinetobacter baumannii* (μg/mL) 34

Figure 3.16. TLC plate 2 of epigallocatechin gallate and 1921D-F7~9 before TLC-agar -overlay bioautography assay 35

Table 3.3. Length of Inhibition Zone (cm) and Retention Factor (Rf) of 1921D-F7~9 in TLC-Agar Overlay Bioautography Assay Against AB5075) 35

Figure 3.17. TLC plates of TLC-agar-overlay bioautography assay after 22-hour incubation 36

Figure 3.18. TLC plates of TLC-agar-overlay bioautography assay after 44-hour incubation 37

Figure 3.19. Reverse-phase TLC plates of 1921D-F7 38

Figure 3.20. Percent cytotoxicity of potent extracts 1921, 1921D and 1921D-F~9. 38

Chapter 1: Introduction

Acinetobacter baumannii

The genus *Acinetobacter* is a diverse group of Gram-negative coccobacilli [1]. Although most species of the genus are non-pathogenic, some of the pathogenic species are causing emerging infectious disease and one of them is *Acinetobacter baumannii*.

1. Spread of *Acinetobacter baumannii* infection

Acinetobacter baumannii first caught people's attention in the 1960s and 1970s by causing infections among soldiers and patients receiving intensive care. Now, it is responsible for about 2-10% of nosocomial infections by Gram-negative bacteria, but the resulting mortality rate ranges from 8% to 35%, and even up to 60% in certain cases [2]. This opportunistic pathogen most often causes ventilation-associated pneumonia, bacteremia, but can also result in skin or soft tissue infection, catheter-associated urinary tract infection, meningitis, endocarditis and ocular infection [2, 3]. If, during early infection, the patient's immune system is not able to clear the bacterium, whether with or without the use of antibiotics, cytokine storm and sepsis syndrome will make treatment even harder [4].

A. baumannii is rarely found in the environment and is not a normal component of the human microbiome. Its natural reservoir is unclear, and it is almost exclusively found in hospitals [2, 5]. As a common nosocomial pathogen, it easily spreads between patients through hands of healthcare workers and contaminated surfaces. The amount of *A. baumannii* shed by infected patients is relatively low but was determined to be enough to cause further infection according to previous

studies [6]. In some cases, aerosol particles from infected patients were found to be the source of infection [4]. Besides healthcare-associated infection, community-acquired *A. baumannii* infection was also reported. Although it mostly affects patients with underlying medical conditions like alcohol abuse, diabetes and cancer, community-acquired infection actually may lead to worse prognosis compared to nosocomial infection [2, 3].

2. Virulence of *Acinetobacter baumannii*

The intrinsic characteristics of the bacterium – tolerance to desiccation and disinfection, motility and formation of biofilm – help with its survival and transmission within the healthcare system. During desiccation, the water in the bacterium is maintained by its outer membrane and its extracellular capsule. Instead of entering a dormant state, the bacterium is kept viable in dry conditions and thus is still capable of colonizing human tissues. Its tolerance to common disinfectant also makes eradication more difficult. Previous studies have shown that low concentration of ethanol promotes the growth and virulence of *A. baumannii*. The bacterium can also produce enzymes to degrade hydrogen peroxide and efflux pumps to clear chlorhexidine. The formation of biofilm further sustains the bacterium on both abiotic and biotic surfaces. Besides providing protection, the ability to form biofilm is also usually linked to higher virulence. The bacterium can also move via twitching motility mediated by type IV pili or via surface-associated motility facilitated by quorum sensing, both of which help with its dissemination [3]. For these reasons, it is not surprising that the bacterium can survive on surfaces for up to 4-5 months, and that most of the *A. baumannii* outbreaks were later determined to be derived from contaminated

fomites in hospitals [6].

3. Antimicrobial-resistant *Acinetobacter baumannii*

Despite the wider and wider spread of *A. baumannii* around the world, the number of effective medications against it is decreasing because of its broad resistance against antibiotics. About 45% of the isolated clinical strains are multiple-drug resistant, and this proportion reaches 70% in Latin America and the Middle East [2]. The flexible genome of *A. baumannii* enables exchange of resistance genes through horizontal gene transfer. This is supported by the fact that many of the genes coding for resistance in *A. baumannii* are flanked by segments of integrases, transposases or insertion sequences, indicating recombination events had happened [2]. During periods of desiccation, the enzyme RecA is upregulated to mediate the recombination and repair of *A. baumannii* genome damaged by loss of water. In this process, the mutation rate is increased by about 50-fold, allowing more resistant genes to arise [3]. Some environmental *Acinetobacter* strains were found to be reservoirs of resistant genes, from which pathogenic strains like *A. baumannii* can preserve and gain even more resistance. For these reasons, a large portion of *A. baumannii* strains are determined to be multiple-drug resistant (MDR) or even extensively-drug resistant (XDR). A strain is determined to be extensively-drug resistant, when it has resistance to all available first-line antibiotics except for ones that are less effective or have higher toxicity [4].

Carbapenem is usually the first-line antibiotic used to treat *A. baumannii* infection, and strains that are resistant to carbapenem are usually resistant to most other antibiotics. Therefore, resistance to carbapenem is usually the hallmark for an *A. baumannii* strain to be determined as extensively-

drug resistant. As well, since the 1990s, carbapenem-resistant *A. baumannii* strains have appeared and rapidly spread around the world, and are not only isolated from patients, but also from cattle and other animals [2, 5].

Now that more and more MDR *A. baumannii* strains have appeared, healthcare providers have turned to antibiotics like colistin, minocycline and tigecycline, which have known side effects of neurotoxicity and nephrotoxicity [7]. Colistin targets lipid A of lipopolysaccharide in the outer membrane of *A. baumannii*, but resistance to colistin has already appeared in strains that have altered or missing lipid A target site [3, 8]. In response to such a broad resistance, healthcare providers now turn to the use of antibiotic combination therapy. For example, the combination of colistin and rifampicin significantly reduces the time needed to clear the bacterium from patients compared to using colistin alone [7]. However, given the frequent gene transmission between strains, combination therapy might fail in the foreseeable future as well.

As the situation of antimicrobial resistance is getting worse, searching for more effective drugs against *A. baumannii* infection is necessary. Potential new treatments include phage therapy, phototherapy, passive vaccination and natural herbal products. One such promising herbal extraction is oleanolic oil [4]. The focus of this research is to investigate the potential of deriving chemicals from medicinal plants to be used as effective treatment against *A. baumannii*. Two strains of *A. baumannii* used for testing in this research were ATCC 17978 and AB5075. The strain ATCC 17978 was isolated in 1951. It is susceptible to antibiotics since it lacks many resistant genes that appeared and accumulated in the 70 years after its isolation [2, 3]. The strain AB5075 is more representative of strains isolated in clinical settings today. It is highly virulent and carries

resistance for multiple antibiotics; thus, the mortality rate is significantly higher upon infection with this strain. The strain is commonly used in laboratories because of its similarity to clinical samples and its susceptibility to tetracycline and hygromycin, which enables it to be genetically modified for testing [9].

***Rosa* × *damascena* Mill.**

The plant *Rosa* × *damascena* Mill. is commonly known as the Damask rose. It belongs to the Rosaceae family and is a cross between *Rosa gallica* and *Rosa moschata*. It is a perennial shrub with compound leaves and is famous for its fragrant pink flowers. It is distributed in Europe and the Middle East, specifically in regions in Iran, Lebanon and the Isparta region of Turkey [10, 11].

Figure 1.1. The flower of *Rosa* × *damascena* Mill., the Damask rose [12].

1. Traditional use of *Rosa* × *damascena* Mill.

The commercial and medicinal use of the plant is of long history. Extraction of the rose essential oil can be dated back to around late 7th AD in the Middle East [12]. Commercially, the essential oil and the distilled water extracted from the rose are widely used in the cosmetic, perfume and food industries. The edible flower of *Rosa* × *damascena* is added in food for flavor,

in herbal tea, in rose petal jam and syrup [13]. Besides its commercial value, its medicinal properties are well recognized in Lebanon, where it has been traditionally used against various maladies. In Lebanon it is used to relieve gastrointestinal problems like stomachache, lack of appetite and constipation; the rose essential oil is used as a gentle laxative. It is also believed to act as a cardiotonic, antirheumatic, antioxidant and antimicrobial. People take it to relive cough and apply it externally to cure dermatitis [14]. The rose essential oil is also considered a relaxant that heals depression, stress, anxiety and migraine [12].

2. Chemical profile of *Rosa* × *damascena* Mill. flower extract

The composition of *R. damascena* extracts varies depending on the extraction method, the collection time, the region where the plant is cultivated, the climate and other factors. Three common kinds of *R. damascena* extracts are the essential oil, which captures most of the aromatic compounds and the characteristic odor of the plant, the hydrosol and the absolute extract [10, 11].

Chemical compounds usually found in the plant are terpenes, flavonoids, glycosides and anthocyanins, and the medicinal properties of *R. damascena* are generally attributed to its high concentration of phenolic compounds [12]. The essential oil of the rose is mainly composed of terpenes. Using GC-MS, the composition of the essential oil is determined to be mainly: citronellol (35.23%), geraniol (22.19%), nonadecane (13.85%) and nerol (10.26%). The composition of hydrosol is similar to that of the essential oil: citronellol (29.44%), geraniol (30.74%), nerol (16.12%) and phenyl ethylalcohol (23.74%). The absolute extract usually has a significantly higher amount of phenyl ethylalcohol (78.38%), but the rest of the composition is similar: citronellol

(9.91%), geraniol (3.71%) and nonadecane (4.35%). Among the three methods of extraction, the rose absolute has the highest concentration of phenolic compounds (2134.3 ± 91.4 GAE/mg/L^{-1}), followed by the essential oil (839.5 ± 59.5 GAE/mg/L^{-1}) and lastly the hydrosol extract (5.2 ± 0.3 GAE/mg/L^{-1}) [10].

Another type of chemicals present in *R. damascena* are vitamin E compounds, which provide the antioxidant activity of its extracts. These compounds include tocopherol and carotene. Among the essential oil, absolute extract and hydrosol of R. damascena, the absolute extract has the highest concentration of tocopherol and carotene [10].

Besides the three aforementioned extraction methods, compounds in *Rosa* × *damascena* flower can also be extracted using organic solvents. The hydromethanolic extraction of *R. damascena* flower was demonstrated to yield bioactive extracts. In this method, the rose flowers was extracted with 80:20 methanol:water mixture (v/v) [13]. The phenolic compounds present in the extracts were determined by comparing the chromatographic behavior and mass spectra of compounds in the extract and those of known phenolic standards. From the study, 12 major flavonoids were identified but no phenolic acid was found. The flavonoids are all derivatives from kaempferol and quercetin, and the most abundant compound is quercetin-3-O-glucoside [13].

3. Pharmacological properties of *Rosa* × *damascena* Mill. flower extract

Rosa × *damascena* extract was shown to have antimicrobial, antioxidant, antiproliferative and relaxant effect in previous research.

The essential oil of *R. damascena* was demonstrated to inhibit the growth of various Gram-

positive and Gram-negative bacteria through well-diffusion assay, disk-diffusion assay and broth microdilution assay. The bacteria against which *R. damascena* essential oil has shown inhibitory effect include human pathogenic bacteria like *Pseudomonas aeruginosa*, *Staphylococcus aureus* and the plant pathogenic bacterium *Xanthomonas axonopodis* spp. *vesicatoria* [10, 11, 15]. The absolute extract of *R. damascena* showed relatively weaker growth inhibitory effect against *Pseudomonas aeruginosa* and *Staphylococcus aureus* compared to the essential oil, but the hydrosol had no antibacterial effect. The individual composition in the essential oil – citronellol, geraniol and nerol – each alone had better antimicrobial activity than that of the essential oil against *Staphylococcus aureus* and *Escherichia coli* [11]. The growth inhibitory effect was proposed to be mainly due to the high concentration of phenolic compounds in the extracts. For the absolute extract, the high concentration of phenylethyl alcohol was responsible for the antimicrobial effect [10]. The hydromethanolic extract of *R. damascena* demonstrated growth inhibitory effects against clinical strains of *Klebsiella pneumoniae*, *Pseudomonas aeruginosa*, *Acinetobacter baumannii*, *Staphylococcus aureus* and *Enterococcus faecalis*. Using the broth microdilution method as well as the rapid p-iodonitrote-trazolium chloride (INT) colorimetric assay, the minimum inhibitory concentrations were determined to range from 0.625 mg/mL to 10 mg/mL [13]. *R. damascena* extracted using methanol was shown to have antimicrobial effect against 15 species of bacteria in agar well diffusion assays, including *Escherichia coli*, *Klebsiella pneumoniae*, *Pseudomonas aeruginosa*, *Salmonella enteritidis*, *Salmonella typhimurium* and *Staphylococcus aureus* [16]. Ethanol extraction of *R. damascena* could lower the MIC of antibiotics against multidrug-resistant *Pseudomonas aeruginosa* obtained from clinical samples [17]. Although the antimicrobial effect

of *R. damascena* extract is generally believed to result from its high abundance of phenolic compounds, the potent chemical compounds were not isolated or identified.

Other prominent medicinal activity of *R. damascena* flower extract includes antioxidant, antiproliferative and relaxant effects. The rose extracts were determined in previous research to have antioxidant effect from flavonoids, phenolic acid, tocopherol and carotene [10, 13, 16]. *R. damascena* hydromethanolic extract showed antiproliferative activity against cervical and hepatocellular carcinoma tumor cell lines [13]. The ethanolic extraction of *R. damascena* flower depresses activity of mice central nervous system, and its aqueous, ethyl acetate and n-butanol extractions can relax the tracheal smooth muscle of guinea pigs [12].

Although *Rosa* × *damascena* extract was repeatedly demonstrated in previous research to have antimicrobial effect, there is no prior research investigating its effect on multidrug-resistant strains of *Acinetobacter baumannii*, nor characterization of the chemical compounds that exhibit growth inhibition on pathogenic bacteria.

Research questions and project aims

The use of medicinal plants to treat diseases has a long history and is still a common treatment method in many developing countries. Medicinal plant extracts are usually mixtures of chemicals and could contain hundreds of different compounds, which are great sources for novel drug development [11]. The use of natural products or natural product-derived compounds is a good alternative that can reduce the reliance on antibiotics and slow the progress of antibiotic resistance. Using products derived from edible plants can also help with infection related to food-borne

pathogen [13].

In a screening of Lebanese plants brought by Dr. Roula Abdel-Massih to the Quave Lab, the *Rosa* × *damascena* flower extract showed antibacterial activity against *Acinetobacter baumannii*. Continuing the preliminary work of Dr. Abdel-Massih, this research intends to characterize the growth inhibitory activity of *Rosa* × *damascena* flower extract against multidrug-resistant *Acinetobacter baumannii*. It is hypothesized that *Rosa* × *damascena* extracts have growth inhibitory effect on *Acinetobacter baumannii* with low toxicity to humans. The goal is to isolate, identify and characterize the potent compound(s) in the plant extracts.

Chapter 2: Materials and Methods

Overview of bioassay-guided fractionation

The fractionation of *Rosa* × *damascena* flowers extract followed an overall scheme: fractionating the extracts, testing the growth inhibitory activity of the extracts against *Acinetobacter baumannii* strains and analyzing the composition of the extracts. The above procedures were repeatedly performed on the most potent extract fraction(s) until the active compound(s) was isolated.

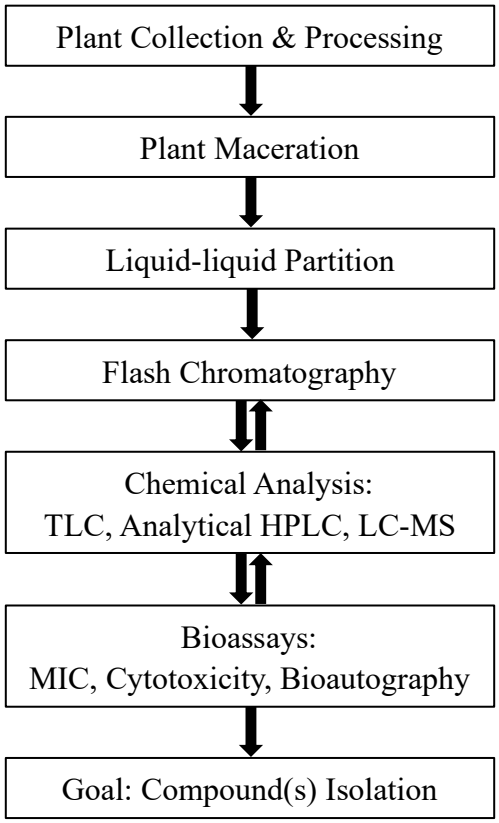

Figure 2.1. The overall scheme of bioassay-guided fractionation of *Rosa* × *damascena* flower extract.

Plant collection and processing

Rosa × *damascena* flowers were collected and dried in Lebanon then shipped to the Quave lab for further processing.

After arriving in the Quave lab, the plant material was first quarantined in a -80 °C freezer to remove any possible pathogens. It was then further air dried and ground into fine powder.

Plant maceration

The plant powder was macerated using 80% ethanol aqueous solution with a ratio of 1 g plant material in 10 mL solution for 72 hours at room temperature with occasional stirring. The maceration was then coarse filtered with Fisherbrand P8 filter paper, followed by fine filtration of the filtrate using Fisherbrand P2 filter paper. The plant material was returned to the container for a second maceration with the same volume of 80% ethanol solution for another 72 hours, which was then double filtered following the same procedure. The plant material was discarded. Via rotary evaporation set at 38 °C, the combined filtrate from the two macerations was concentrated and dried down completely to remove the solvent. Deionized water was added to resuspend the dried material. The water suspension was then shell-frozen and lyophilized for about 24 hours to remove any water. The dried maceration extract was collected from the round bottom flask and weighed, and the yield was calculated using the equation: $yield = \frac{mass\ of\ dry\ material\ obtained\ from\ \ maceration}{mass\ of\ plant\ powder\ used\ to\ make\ maceration} \times 100$. This was the crude extract 1921.

Fractionation of plant extracts

1. Liquid-liquid partition

Liquid-liquid partition of the maceration extract solution was performed to separate chemical compounds in the maceration crude extract based on polarity.

After maceration, dried *Rosa* × *damascena* crude extract was dissolved in less than 20% methanol aqueous solution with a ratio of 1 g extract in 30 mL solvent. In a separatory funnel, the solution was partitioned against hexane, ethyl acetate and water-saturated n-butanol respectively. The solution was partitioned three times using each of the aforementioned organic solvent. The total volume of each organic solvent used was equal to the initial volume of the extract solution. In the first hexane partition, one-third total volume of hexane was first added into the separatory funnel, and the separatory funnel was shaken thoroughly to thoroughly mix hexane and the crude solution. The mixture was left until two separated clear layers formed. The bottom crude layer was drained down into the original flask for subsequent partition, and the top hexane layer was poured from the top into a new flask. After the crude solution was returned to the separatory funnel, it was partitioned two more times with hexane following the same aforementioned procedure. All of the hexane layers were combined. After the third hexane partition, the crude solution was partitioned three times with ethyl acetate, followed by three water-saturated n-butanol partitions. The remaining crude solution was kept as the aqueous layer. The collected hexane, ethyl acetate and n-butanol layers were filtered through Na_2SO_4 to remove water. The hexane layer was air dried after being concentrated via rotary evaporation set at 38 °C; the dried hexane partition extract was

named 1921B. Solvents in ethyl acetate, n-butanol and water layers were removed via rotary evaporation set at 38 °C; the dried material was resuspended in distilled water, shell-frozen and lyophilized, yielding dry partition extracts named 1921C, 1921D and 1921E, respectively. The four partition extracts were weighed, and yields were calculated using $yield = \frac{mass\ of\ dry\ partition\ extract}{mass\ of\ crude\ extract\ used\ in\ partition} \times 100$.

2. Flash chromatography

Flash chromatography was run to prepare fractions of 1921D extract. To prepare the cartridge sample for flash, 1921D extract was dissolved with methanol, and Celite was added to the solution with a ratio of 4 g Celite for every 1 g extract. Methanol was added to create a suspension of Celite in a round bottom flask, after which the solvent was completely removed through rotary evaporation set at 38 °C. The dried mixture of extract and Celite was removed from the round bottom and packed in a cartridge of appropriate size. The packed cartridge was dried in a lyophilizer for at least half an hour, and was taken out right before loading onto the CombiFlash Rf machine. The stationary phase used for separation was a RediSep Rf High Performance Silica 24g Gold column. The mobile phases used were: (A) HPLC-grade chloroform, (B) HPLC-grade methanol; the mobile phases were switched to (A) HPLC-grade methanol and (B) deionized water towards the end of the run. The flow rate was 35 mL/min. The wavelengths of detection were set at 254 nm and 280 nm.

The solution eluted from the flash run was collected using 18 mm ×150 mm test tubes. The solution was then examined with thin layer chromatography. Tubes of solution with similar

chemical compositions was combined into fractions according to the TLC results as well as the flash chromatogram.

Analysis of plant extracts

1. Normal-phase TLC (Thin Layer Chromatography)

Normal-phase thin layer chromatography was performed on extracts 1921C and 1921D to determine the solvent system for subsequent flash chromatography fractionation. The pure solvents tested for mobile phase were methanol, ethanol, isopropyl alcohol, ethyl acetate, hexane, acetone, chloroform, petroleum ether, acetonitrile and tetrahydrofuran. Solutions tested for mobile phases were 50% methanol and 50% ethyl acetate, 90% methanol and 10% water, and 40% methanol and 60% chloroform. After running the thin layer chromatography, the compounds on the plate were visualized using the vanillin/sulfuric acid spraying reagent with heating.

After flash chromatography was ran for 1921D, thin layer chromatography was performed again on the solutions collected from the flash run to analyze the compounds isolated in each tube. The mobile phase used was 40% methanol and 60% chloroform, and the TLC plates were visualized using the same method. Results from the TLC plates were used to guide the combination of 1921D flash fractions.

For the active fractions 1921D-F7, 8 and 9, TLC was performed using 50% methanol and 50% ethyl acetate as mobile phase to compare the chemicals in the three fractions.

2. Analytical HPLC (High Performance Liquid Chromatography)

Reversed-phase analytical HPLC was performed to further separate and analyze the chemicals

within the crude extract 1921 and the partition extracts 1921B~E based on polarity.

Extracts were dissolved in different solvents to make about 0.5-1 mL of 10 mg/mL analytical HPLC samples. The crude maceration extract (1921) and ethyl acetate extract (1921C) were dissolved in methanol, hexane extract was dissolved in 80% methanol and 20% isopropyl alcohol solution, and n-butanol (1921D) and aqueous layers (1921E) were dissolved in 75% methanol and 25% DI water. From the prepared samples, 25 μL was injected into the HPLC machine and run through an Agilent Eclipse XDB-C18 column (250×4.6 mm, 5 μm with or without matching guard column) at 35 °C. The mobile phases used were: (A) 0.1% formic acid in DI water, (B) 0.1% formic acid in acetonitrile, with a flow rate of 1.000 mL/min. The wavelengths used for detection were: 217, 254, 280, 314, 360, 420 and 550 nm, with no reference wavelength. The gradient of mobile phase was shown as follow:

Time (min)	A (%)	B (%)
10.00	95.0	5.0
60.00	65.0	35.0
70.00	0.0	100.0
80.00	0.0	100.0
80.01	95.0	5.0
90.00	95.0	5.0

HPLC was performed again on the active flash fractions to guide further separation. Flash fractions 1921D-F7~9 were dissolved in methanol with a concentration of 10 mg/mL, from which 10 μL was injected. The column, flow rate and detected wavelengths were kept unchanged. The gradient of mobile phase was the same as the aforementioned method used for extracts 1921 and 1921B~E.

3. LC-MS (Liquid Chromatography-Mass Spectrometry)

LC-MS was performed on the 1921D fraction and the active flash fractions 1921D-F7~9. The LC-MS solution sample was prepared in MS-grade methanol, reaching a final concentration of 10 mg/mL. Mass spectrometry of the four samples was performed in both positive and negative mode. For extract 1921, 25 μL was injected; for the other extracts, 10 μL were injected. The extracts were run through an Agilent Eclipse XDB-C18 column (250×4.6 mm, 5 μm with or without matching guard column) at 35 °C. The mobile phases used were: (A) 0.1% formic acid in DI water, (B) 0.1% formic acid in acetonitrile, with a flow rate of 1.000 mL/min. After method optimization, the gradient of mobile phase was modified to be:

Time (min)	A (%)	B (%)
5.00	95.0	5.0
65.00	75.0	25.0
75.00	0.0	100.0
80.00	0.0	100.0
80.01	95.0	5.0
100.00	95.0	5.0

4. Reverse-phase TLC (Thin Layer Chromatography)

Reverse-phase thin layer chromatography was performed on extract 1921D-F7~9 to optimize separation of these extracts, so that more information can be obtained from the TLC-agar-overlay bioautography assay. The tested mobile phase systems were shown below [18]. The obtained TLC plates were not treated with vanillin/sulfuric acid spray reagent and were viewed under UV.

Table 2.1. Mobile phase tested for reverse-phase TLC of extracts 1921D-F7~9		
Mobile Phase	Solvents	Solvent ratio (v:v)
1	acetonitrile:water	15:85
2	acetonitrile:water	30:70
3	acetonitrile:water	50:50
4	methanol:water	30:70
5	toluene:ethyl acetate	95:5
6	chloroform:methanol:water	70:30:4
7	ethyl acetate:acetic acid:formic acid:water	100:11:11:27
8	acetonitrile:water:formic acid	30:8:2
9	n-butanol:acetic acid :water	7:1:2

Bioactivity assays

1. Broth microdilution MIC assay on 1921, 1921B, C, D and E

Broth microdilution MIC assay was performed on crude extract 1921, and partition extracts 1921B, C, D, and E using ESKAPE pathogens in 96-well flat bottom plate. The bacteria strains used were summarized in the table below.

Table 2.2. ESKAPE pathogen strains used in broth microdilution MIC assay of extracts 1921 and 1921B~E	
Strain	**Species**
ATCC 17978	*Acinetobacter baumannii*
AB5075	*Acinetobacter baumannii*
CDC32	*Enterobacter cloacae*
AH0071 (PAO1)	*Pseudomonas aeruginosa*
EU32	*Klebsiella pneumoniae*
EU49	*Enterococcus faecium*
AH1263	*Staphylococcus aureus*

Bacteria was cultured overnight in 6 mL CAMHB (cation-adjusted Mueller Hinton Broth) at 35 °C with continuous shaking at an angle at 200 rpm, and standardized at OD590 to a cell density of 0.0006 (5×10^5 CFU/mL). The medium used was CAMHB (cation-adjusted Mueller Hinton

Broth), vehicle control was DMSO, antibiotic control was Gentamicin, and a blank medium control was also included. Each concentration of extracts and controls was tested in triplicate. In a sterile 96-well flat bottom plate, the final volume of each well was 400 µL. Extracts were dissolved in DMSO to make 20 mg/mL stock solution. The tested samples were two-fold diluted to reach final concentrations from 512 µg/mL to 16 µg/mL. The highest extract concentration, 512 µg/mL, was obtained by adding 10.24 µL extract solution and 389.76 µL of working culture (standardized bacteria and CAMHB) in the first column of wells. To the remaining wells, only 200 µL of working culture was added. Two-fold serial dilution was performed by adding 200 µL mixture from the previous column of wells into the next column of wells using a multi-channel pipette. The positive control Gentamicin was two-fold serial diluted starting from 64 µg/mL. After adding the extract samples, medium, bacterial culture and controls, the plate was read under OD600 nm before incubation. Except for ATCC 17978 and AB0575, which were incubated for 22 hours, CDC32, AH0071, EU32, EU49, and AH1263 were incubated for 18 hours at 35 °C. The plates were read again after incubation.

The percent inhibition was calculated using $\%\, inhibition = (1 - \frac{ODt18 - ODt0}{avg(ODvc18 - ODvc0)}) \times 100$. ODvc18 is the OD600 reading for the vehicle control after 18 hours of incubation; ODvc0 is the reading for the vehicle control before incubation. ODt18 is the OD600 read for each extract concentrations 18 hours (22 hours for *Acinetobacter baumannii* strains) after incubation; ODt0 is the reading for the respective extract treatments before incubation. The minimum inhibitory concentration (MIC) is determined to be the lowest concentration that showed 90% inhibition of the bacterial growth, and IC50 is the lowest concentration that showed 50% inhibition of the

bacterial growth.

2. Broth microdilution MIC assay on 1921D flash fractions

Broth microdilution MIC assay was performed on flash fractions of the active extract 1921D in a 96-well flat bottom plate. The tested extract concentrations were 256, 128, 64, 32, 16 and 8 μg/mL following two-fold dilution. Extract samples were prepared by dissolving extracts in DMSO to make 10 mg/mL stock solution. The bacterial strains used were ATCC 17978 (*Acinetobacter baumannii*) and AB0575 (*Acinetobacter baumannii*), with Gentamicin as the antibiotic control, DMSO as the vehicle control and CAMHB as the medium control. The same procedure for broth microdilution MIC assay of 1921 extracts was used to determine the MIC of the 1921D fractions.

3. Cytotoxicity assay

LDH cytotoxicity testing was performed on extracts 1921, 1921D, 1921D-F7~9 to determine whether the extracts that showed growth inhibitory effect against multidrug-resistant *A. baumannii* demonstrate inhibitory effect on growth of human skin cells. The cells used were human immortalized keratinocytes (HaCaT), which were cultured under 37 °C and 5% CO_2 in Dulbecco's modified Eagles' medium (DMEM) supplemented with 4.5 g/L glucose, 10% fetal bovine serum, 100IU Penicillin and 100 μg/mL Streptomycin. For the cytotoxicity assay, the cell culture was standardized to 4×10^4 cells/mL. In a 96-well tissue culture treated flat bottom microtiter plate, 200 μL of the standardized cell culture was added and incubated under 37 °C and 5% CO_2 for 48 hours. After incubation, 200 μL of supplemented DMEM and the tested extracts of various concentrations

were added into each well. The tested extracts were dissolved in DMSO to make 50 mg/mL stock solution, which were 2-fold serial diluted to concentrations from 512 μg/mL to 4 μg/mL for the cytotoxicity assay. The positive control was 20 μL of lysis buffer, and the negative control was DMEM. The extracts were tested in triplicate. After incubation under 37°C and 5% CO_2 for 24 hours, lactate dehydrogenase (LDH) assay was performed to the cells, and the optical density was measured to determine the lysis of cells. Cytotoxicity was calculated using: $\%\, cytotoxicity = \frac{OD\ extract - OD\ spontaneous}{OD\ maximum} \times 100$, with OD spontaneous obtained from the negative control and OD maximum from the positive control.

4. TLC-agar-overlay bioautography assay

TLC-agar-overlay bioautography assay was performed on extracts 1921D-F7~9 to elucidate the active fractions of these extracts for further separation. Normal-phase TLC was run for 1921D-F7~9 with 60% methanol and 40% ethyl acetate as the mobile phase. The standard used for standardization of retention factor (Rf) was epigallocatechin gallate, which was also run with the extracts on each TLC plate. A total of four TLC plates were ran, with two plates running at one time. The TLC plates were dried thoroughly and visualized under UV to check if there were significant variation between plates. Pictures of TLC plate number two were taken under UV as well as visible light, and the Rf values of epigallocatechin gallate as well as 1921D-F7~9 were calculated according to the equation: $Rf = \frac{the\ max\ length\ between\ start\ point\ and\ compound}{length\ between\ start\ point\ and\ solvent\ front}$.

The bacteria used in the assay was AB5075 genetically modified with the insertion of a LacZ gene. Liquid overnight culture of the bacterium was prepared in LB broth and incubated under

35 °C with continuous shaking at an angle at 200 rpm. Soft LB agar was prepared by adding 0.5% agar in LB broth. The overnight liquid culture was standardized at OD590 nm to a cell density of 0.0006 (5×10^5 CFU/mL). When the autoclaved soft LB agar cooled down to near body temperature, an appropriate amount of liquid culture and X-gal were added to meet a ratio of 100 µL X-gal per 20 mL LB soft agar. The materials were mixed thoroughly with stirring on a stir plate. Three TLC plates were put into three 15-mL petri dishes, then the agar mixture was poured into the petri dishes covering the whole TLC plates. After the soft agar solidified, the plates were incubated upright under 35ºC for 22 hours. Pictures of the petri dishes were taken, and the zones of inhibition were measured. The plates were incubated for another 22 hours, and then set of measurements were taken.

Chapter 3: Results

Overall fractionation scheme

The overall isolation process identified the *Rosa* × *damascena* extracts that demonstrated the most growth inhibition against *Acinetobacter baumannii* strains ATCC 17978 and AB5075 according to MIC results from broth microdilution assays (Figure 3.1).

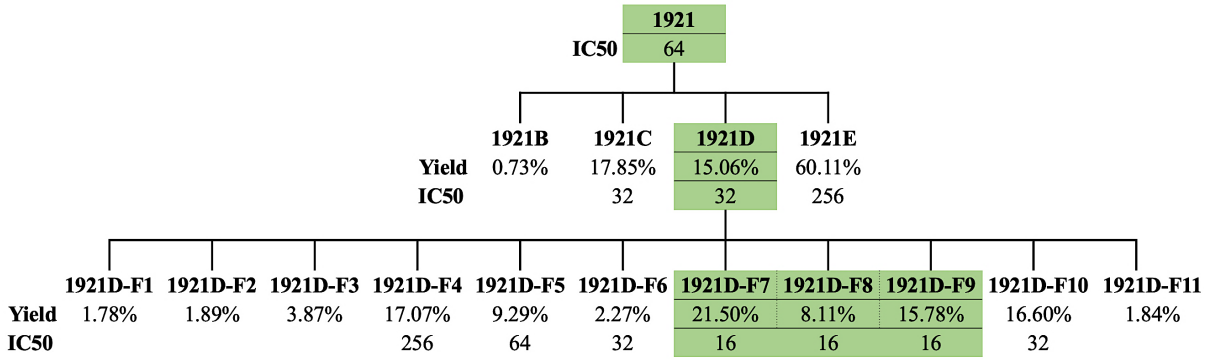

Figure 3.1. Parent-child tree of the isolation scheme of *Rosa* × *damascena* flower extract. Extracts that were studied in the research are highlighted. The IC50 values were obtained from broth microdilution MIC assay of the extracts against *A. baumannii* strains ATCC 17978 and AB5075; each extract showed the same IC50 against both strains. Extracts without IC50 indicated didn't reach 50% inhibition.

Extracts 1921 and 1921B~E

1. Analytical HPLC

The analytical HPLC run of the crude and partition extracts yielded chromatograms with separated peaks of absorbance under wavelength of 280 nm. The majority of the peaks for extracts 1921, 1921C, 1921D and 1921E were distributed at regions with low concentration of solvent B, acetonitrile (Figure 3.2, 4-6.). One exception is extract 1921B, in whose chromatogram most of the peaks were clustered towards the region with high acetonitrile concentration (Figure 3.3).

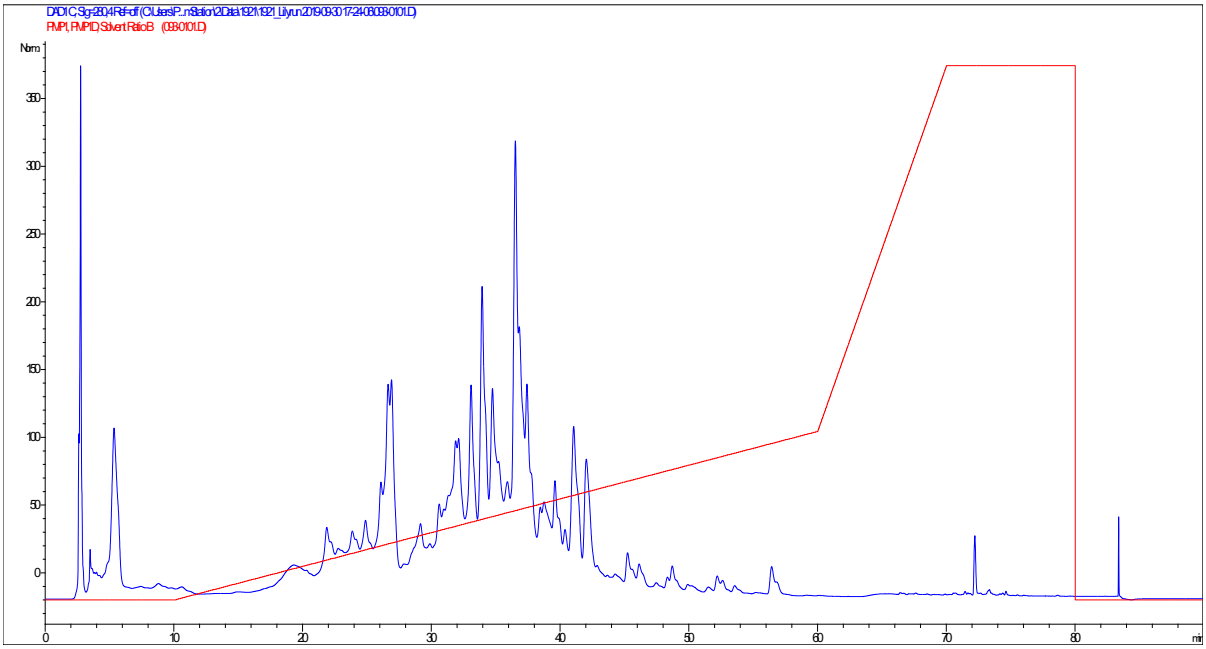

Figure 3.2. Analytical HPLC chromatogram of extract 1921 obtained under 280 nm with %B gradient overlaid. 1921 is the crude extract of *Rosa* × *damascena*. The solvent system is: (A) 0.1% formic acid in deionized water, (B) 0.1% formic acid in acetonitrile.

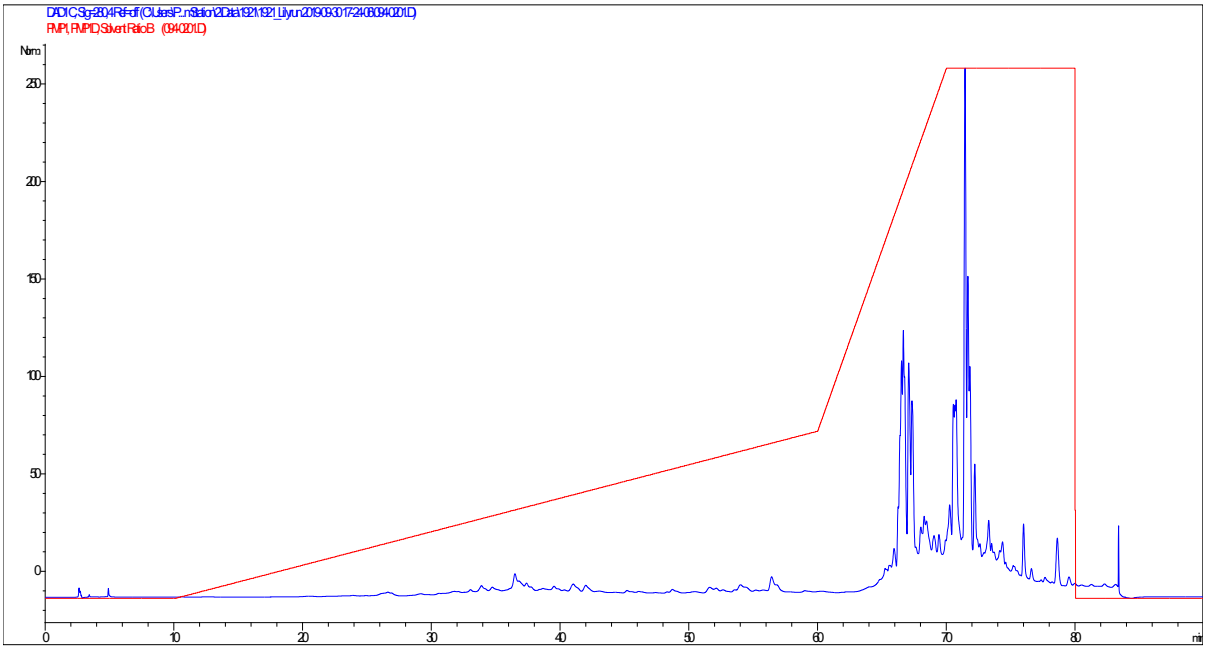

Figure 3.3. Analytical HPLC chromatogram of extract 1921B obtained under 280 nm with %B gradient overlaid. 1921B is the hexane partition extract of *Rosa* × *damascena*. The solvent system is: (A) 0.1% formic acid in deionized water, (B) 0.1% formic acid in acetonitrile.

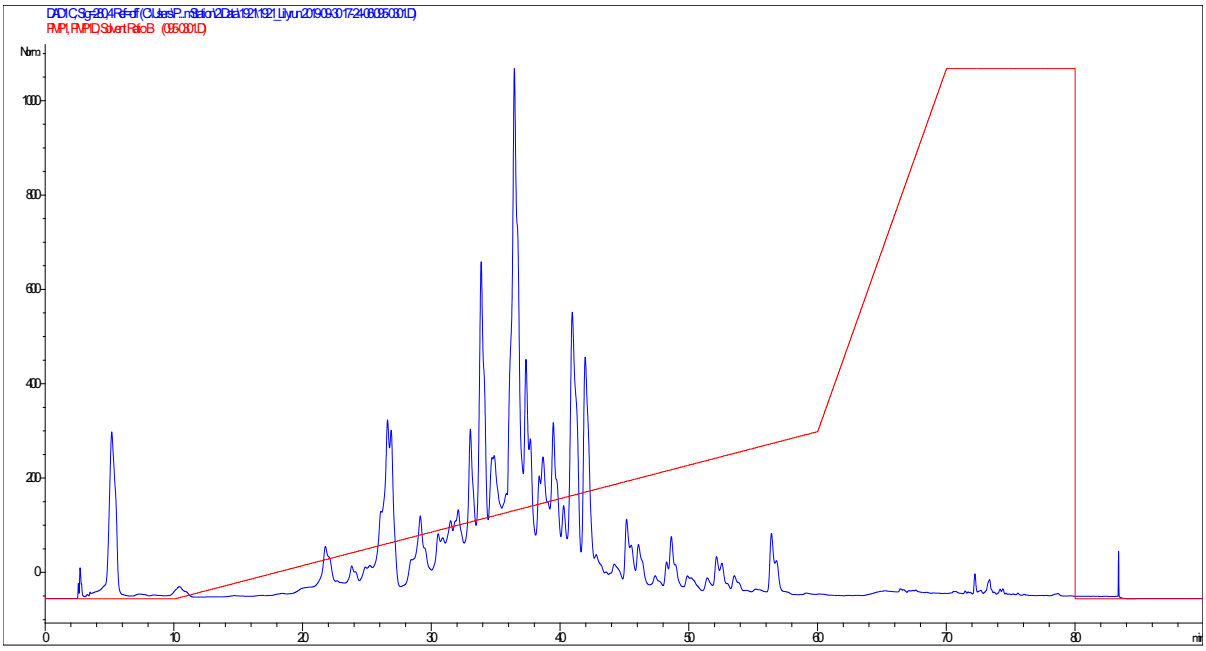

Figure 3.4. Analytical HPLC chromatogram of extract 1921C obtained under 280 nm with %B gradient overlaid. 1921C is the ethyl acetate partition extract of *Rosa* × *damascena*. The solvent system is: (A) 0.1% formic acid in deionized water, (B) 0.1% formic acid in acetonitrile.

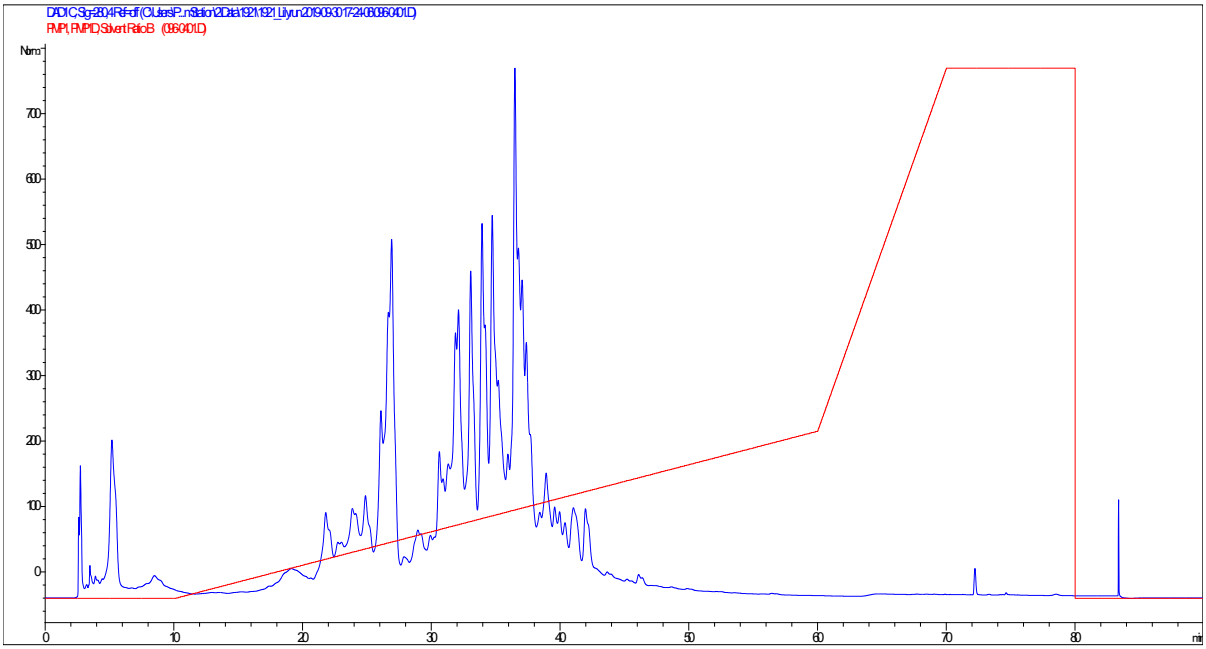

Figure 3.5. Analytical HPLC chromatogram of extract 1921D obtained under 280 nm with %B gradient overlaid. 1921D is the water-saturated n-butanol partition extract of *Rosa* × *damascena*. The solvent system is: (A) 0.1% formic acid in deionized water, (B) 0.1% formic acid in acetonitrile.

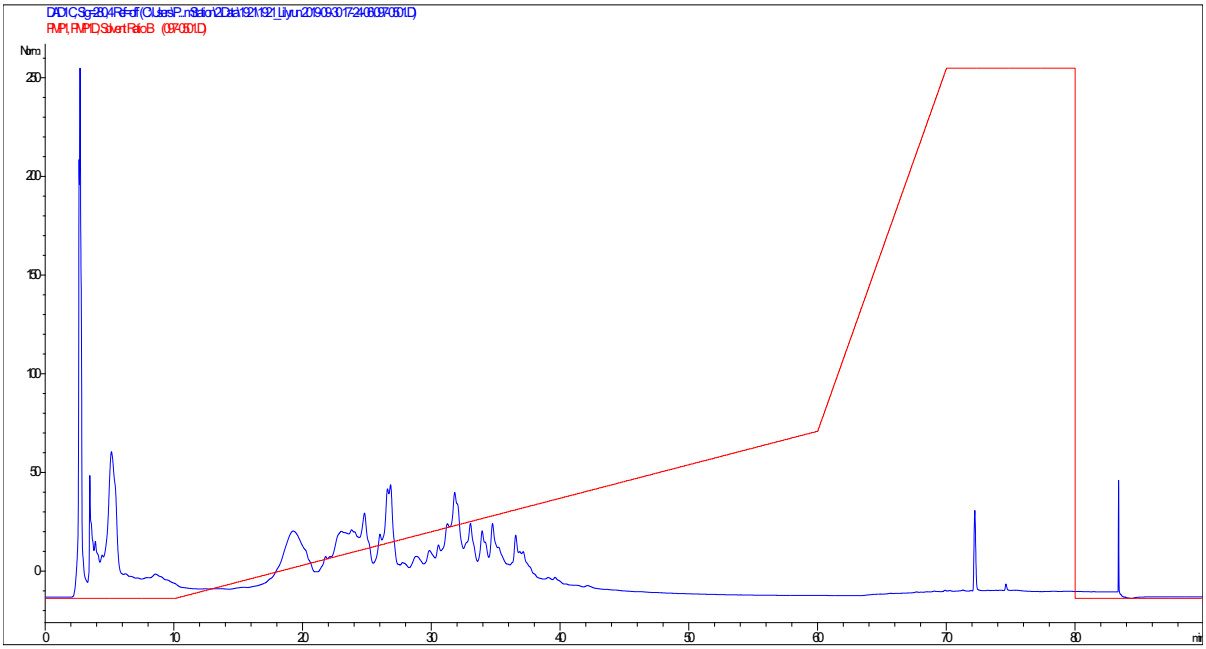

Figure 3.6. Analytical HPLC chromatogram of extract 1921E obtained under 280 nm with %B gradient overlaid. 1921E is the aqueous partition extract of *Rosa* × *damascena*. The solvent system is: (A) 0.1% formic acid in deionized water, (B) 0.1% formic acid in acetonitrile.

2. Broth microdilution MIC assay against ESKAPE Pathogens

Growth inhibition curves of the extracts against ESKAPE pathogens were plotted from data obtained from the broth microdilution MIC assay. Average and standard deviation of percent of inhibition was calculated for each of the triplicates (Figure 3.7).

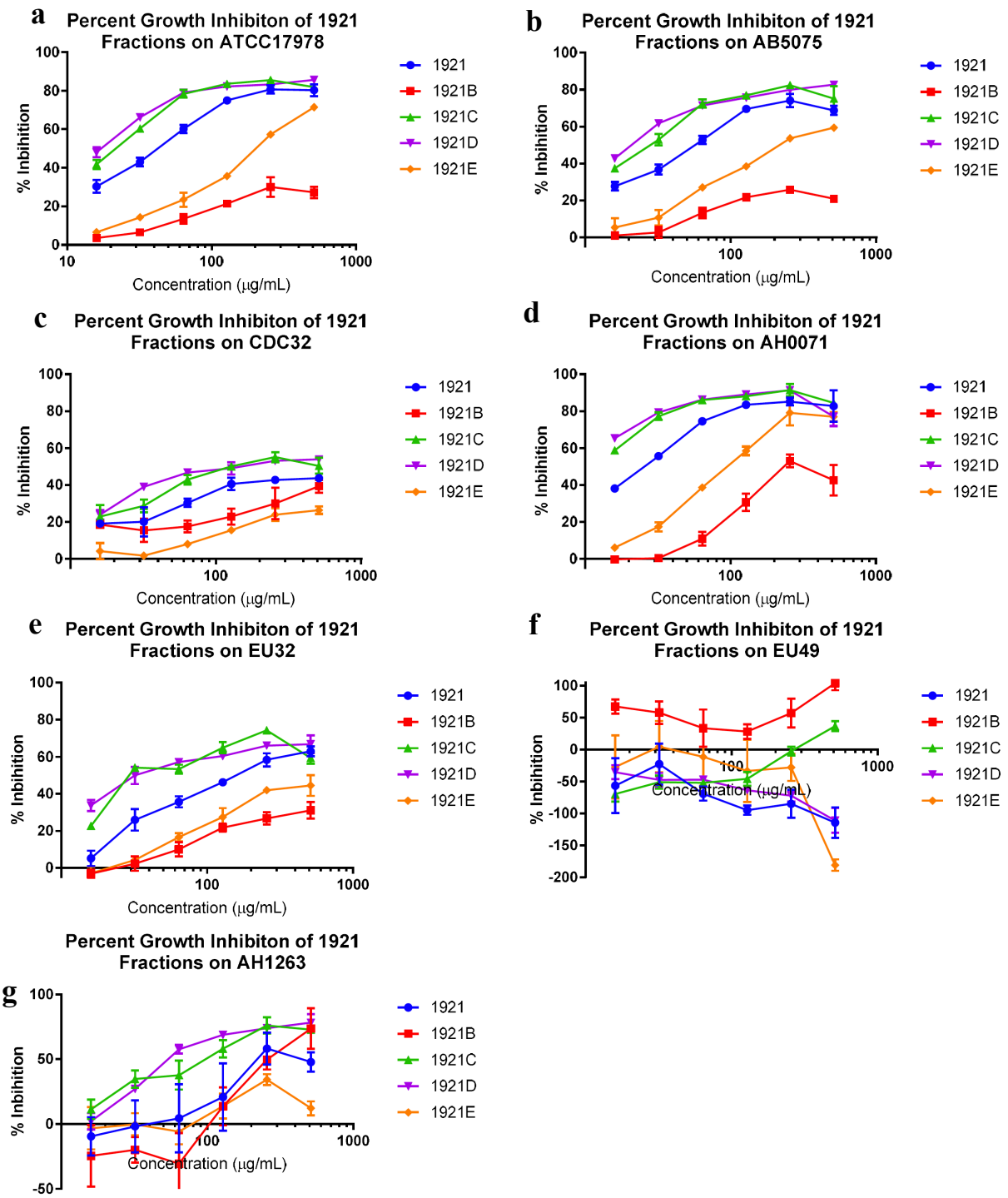

Figure 3.7. Percent growth inhibition of *Rosa* × *damascena* crude and partition extracts against ESKAPE pathogens. ESKAPE pathogens used: a. *Acinetobacter baumannii*, b. *Acinetobacter baumannii*, c. *Enterobacter cloacae*, d. *Pseudomonas aeruginosa* (PAO1), e. *Klebsiella pneumoniae*, f. *Enterococcus faecium*, g. *Staphylococcus aureus*. The x-axis is in log-10 scale. The error bar represents standard deviation within triplicate.

IC50 value was determined to be the concentration where 50% growth inhibition of the bacterium is achieved (Table 3.1).

Table 3.1. IC50 of 1921 and 1921B~E against ESKAPE Pathogens (μg/mL)

	ATCC 17978	AB5075	CDC32	AH0071	EU32	EU49	AH1263
1921	64	64	--	32	256	--	256
1921B	--	--	--	256	--	--	512
1921C	32	32	128	--	32	--	128
1921D	32	32	256	--	64	--	64
1921E	256	256	--	128	32	256	--

Extracts 1921D and 1921D-Fs

1. Flash chromatography

From the flash chromatography run of the chosen potent extract 1921D, a total of 168 test tubes of solution were produced. According to the results of TLC and chromatogram, they were recombined into 11 fractions: 1921D-F1 (tubes 1-15), 1921D-F2 (tubes 16-21), 1921D-F3 (tubes 22-32), 1921D-F4 (33-41), 1921D-F5 (tubes 42-46), 1921D-F6 (tubes 47-48), 1921D-F7 (tubes 49-73), 1921D-F8 (tubes 74-92), 1921D-F9 (tubes 93-117), 1921D-F10 (tubes 118-140) and 1921D-F11 (tubes 141-168).

The flash chromatograms showed separated peaks of absorbance under wavelength 280 nm. The first three major peaks were distributed in three distinct isocratic concentrations of the initial solvent system: at 80% chloroform and 20% methanol, 70% chloroform and 30% methanol, 60% chloroform and 40% methanol. The last peak appeared in the range of 40% to 100% methanol, and there were two crests within the last peak. No peak appeared after the switch of solvent system (Figure 3.8).

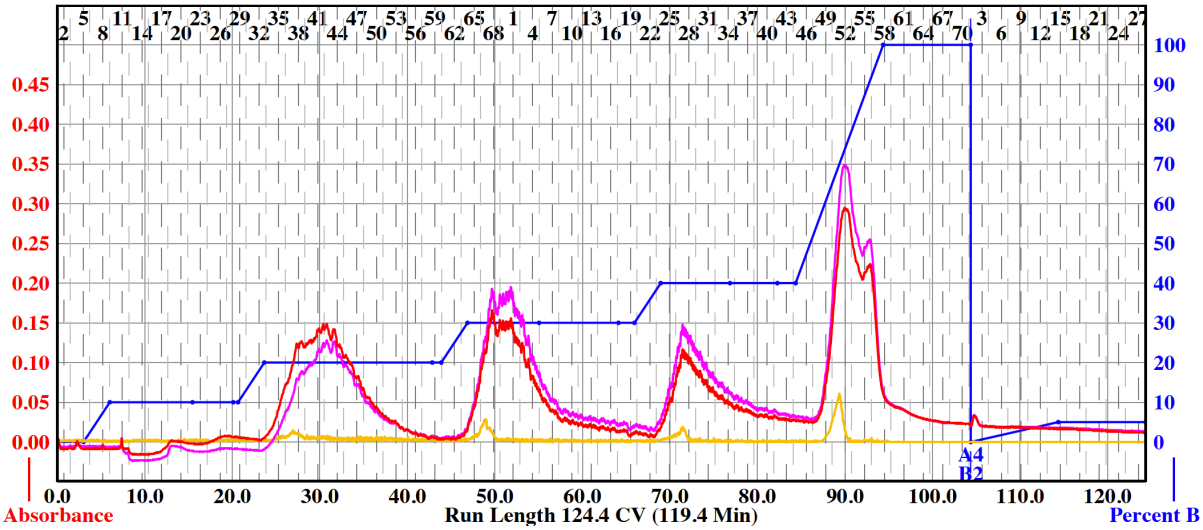

Figure 3.8. Flash chromatogram of 1921D obtained under 280 nm with %B gradient overlaid. The initial solvent system is: (A) chloroform, (B) methanol; the solvent system was switched were switched at around 105.0 CV to: (A) methanol, (B) deionized water.

2. TLC Plates for 1921D flash fractions

The solutions obtained from the flash run of 1921D were analyzed with normal-phase TLC for recombination. TLC was performed for solutions in tube 1-75. No visible mark was seen on the TLC plate for tubes 1-15. One mark near the solvent front was observed on the TLC plate for tubes 16-21. Two spots with clear separation were visible near the solvent on the TLC plate for tubes 22-32. On the TLC plate for tubes 33-41, there were two marks near the solvent front and one mark near the start line. On the TLC plate for tubes 42-46, there was only one mark near the solvent front and one mark near the start line. The mark near the solvent front disappeared and only the mark near the start line could be seen on the TLC plate for tubes 47-48. Starting from tube 49, the samples became harder to separate and stayed close to the start line; from tube 58 on, the samples stick to the start line (Figure 3.9). No TLC was performed for solutions in the rest of the tubes. Based on the above TLC results as well as the chromatogram, test tubes of solution obtained from

flash chromatography were combined into 11 flash fractions.

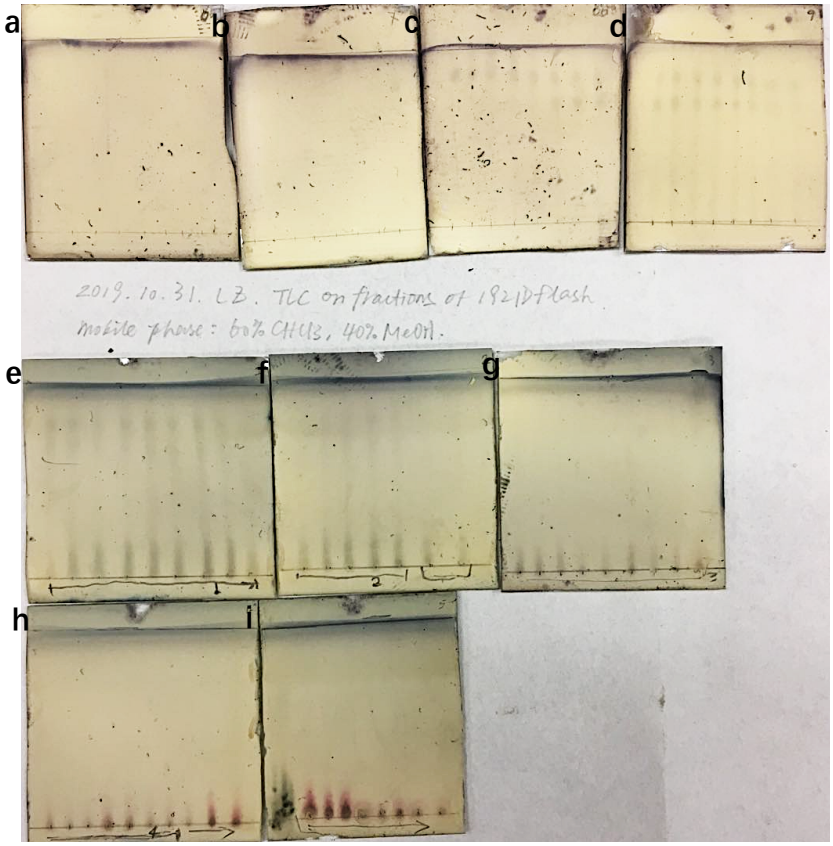

Figure 3.9. Normal-phase TLC of 1921D flash solutions. The mobile phase was 40% methanol and 60% chloroform. The TLC plates were visualized with vanillin/sulfuric acid spraying reagent under: visible light. The solutions run on each TLC plate are: a. tubes 1-8, b. tubes 9-16, c. tubes 17-24, d. tubes 25-32, e. tubes 33-41, f. tubes 42-48, g. tubes 49-57, h. tubes 58-67, i. tubes 68-75.

Extracts 1921D-F7~9

1. Normal-phase TLC

Normal-phase TLC was performed for the active extracts 1921D and 1921D-F7~9 to compare their chemical compositions. From visualization using vanillin/sulfuric acid reagent as well as under UV, extract 1921D exhibited at least five distinct bands. Extract 1921D-F7 showed at least four bands, 1921D-F8 had at least two bands, and 1921D-F9 had at least two bands.

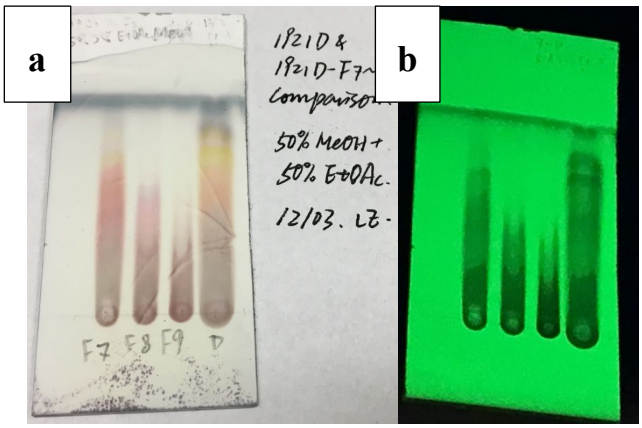

Figure 3.10. Normal-phase TLC of 1921D and 1921D-F7~9. The mobile phase was 50% methanol and 50% ethyl acetate. The TLC plates were visualized with vanillin/sulfuric acid spraying reagent under: a. visible light, b. UV light.

2. Analytical HPLC

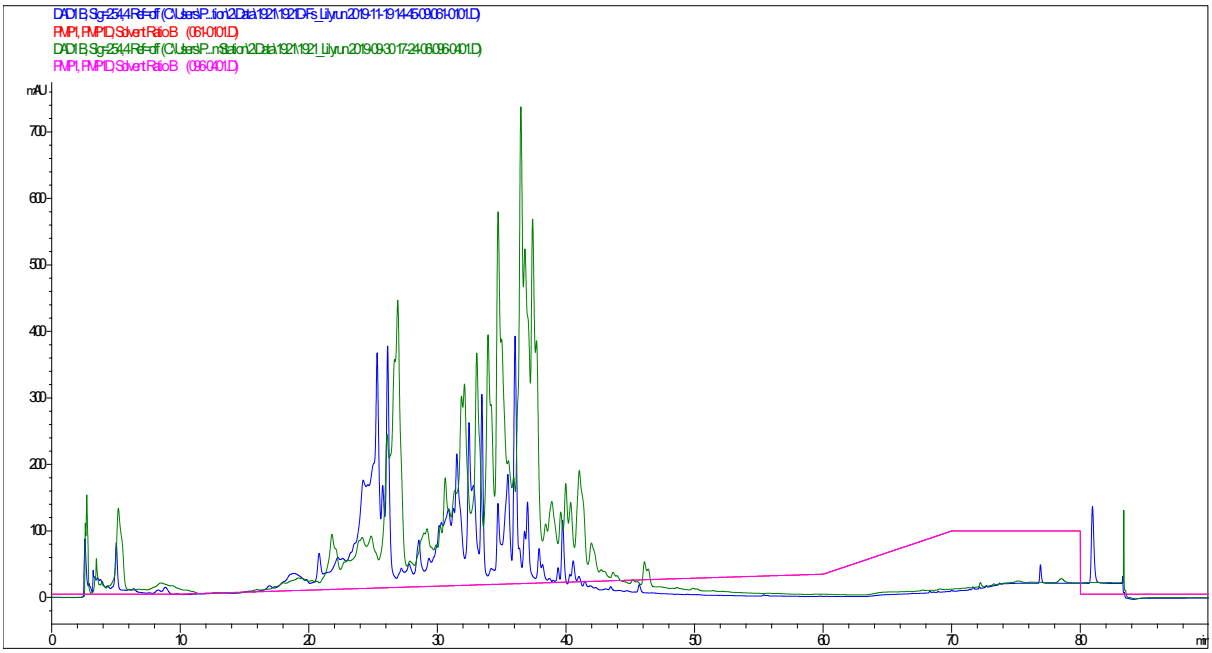

Figure 3.11. Analytical HPLC chromatogram of extracts 1921D-F7 and 1921D obtained under 254 nm with %B gradient overlaid. 1921D-F7 is the 7th recombined flash fraction of extract 1921D. The solvent system is: (A) 0.1% formic acid in deionized water, (B) 0.1% formic acid in acetonitrile. The blue line is 1921D-F7 and the green line is 1921D.

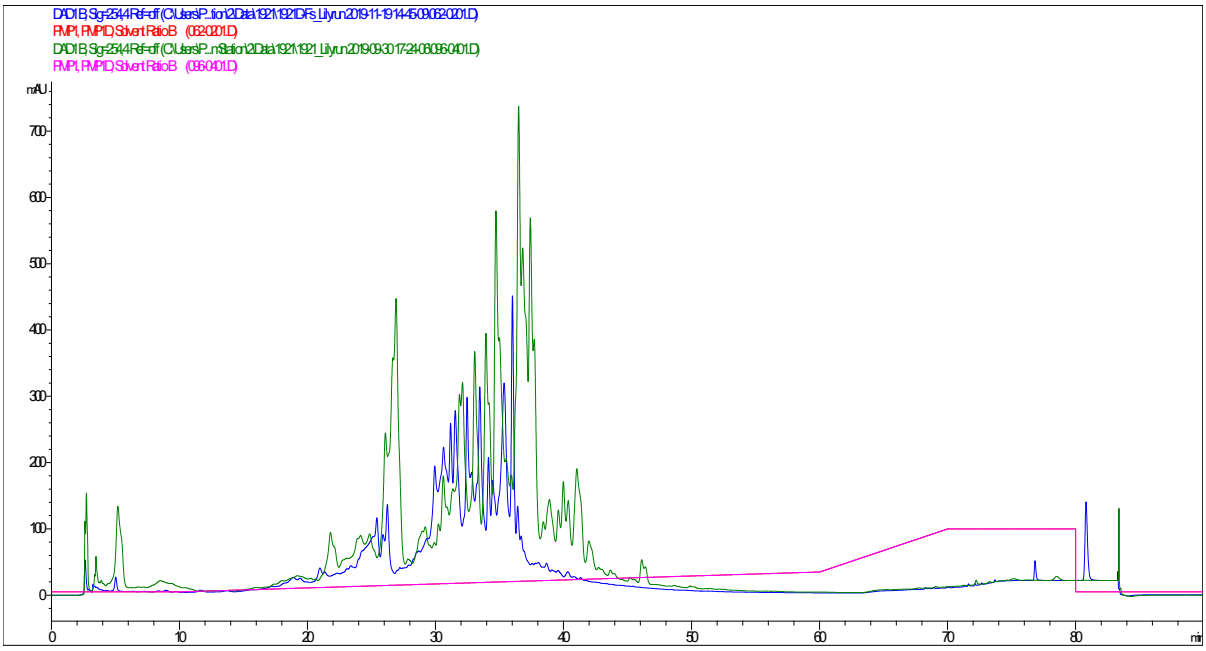

Figure 3.12. Analytical HPLC chromatogram of extracts 1921D-F8 and 1921D obtained under 254 nm with %B gradient overlaid. 1921D-F8 is the 8th recombined flash fraction of extract 1921D. The solvent system is: (A) 0.1% formic acid in deionized water, (B) 0.1% formic acid in acetonitrile. The blue line is 1921D-F8 and the green line is 1921D.

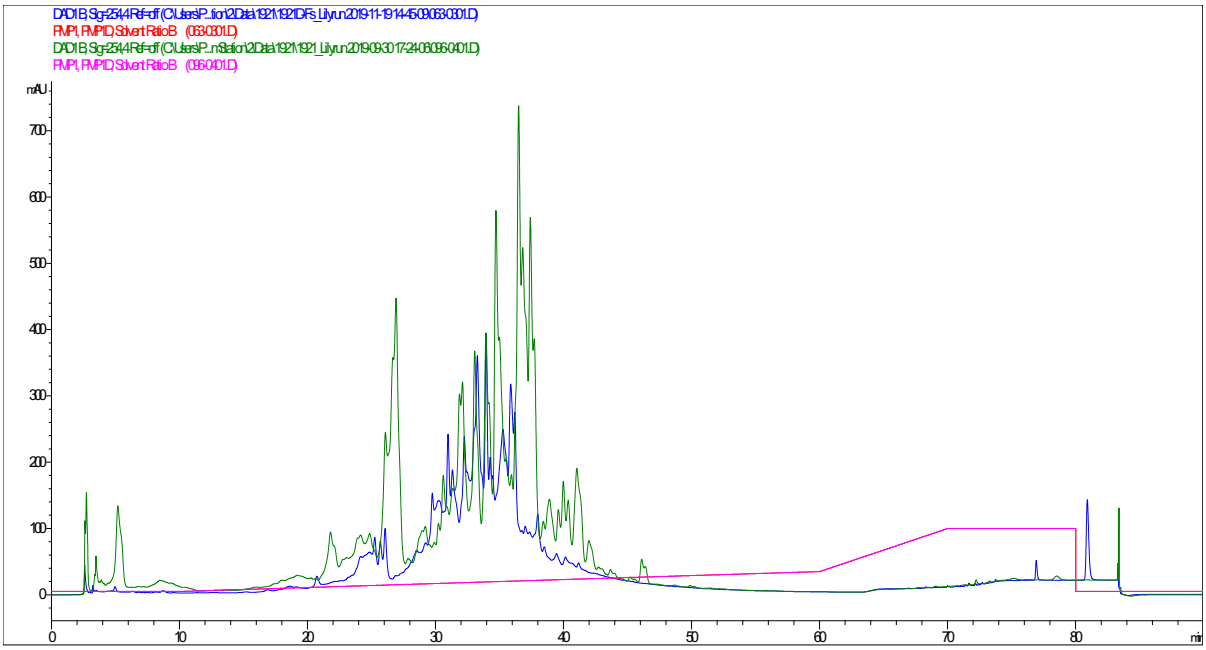

Figure 3.13. Analytical HPLC chromatogram of extracts 1921D-F9 and 1921D obtained under 254 nm with %B gradient overlaid. 1921D-F9 is the 9th recombined flash fraction of extract 1921D. The solvent system is: (A) 0.1% formic acid in deionized water, (B) 0.1% formic acid in acetonitrile. The blue line is 1921D-F9 and the green line is 1921D.

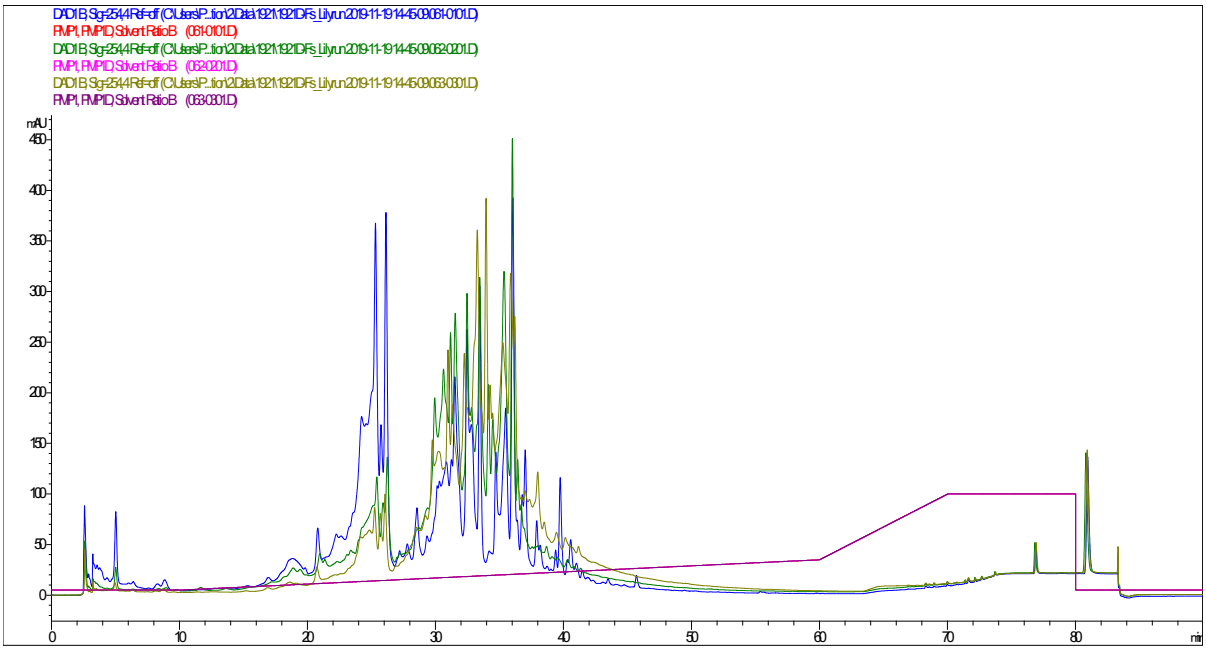

Figure 3.14. Analytical HPLC chromatogram of extracts 1921D-F7~9 obtained under 254 nm with %B gradient overlaid. 1921D-F7~9 is the 7~9th recombined flash fractions of extract 1921D. The solvent system is: (A) 0.1% formic acid in deionized water, (B) 0.1% formic acid in acetonitrile. The blue line is 1921D-F7, the green line is 1921D-F8, and the brown line is 1921D-F9.

3. Broth microdilution MIC assay against *Acinetobacter baumannii*

Growth inhibition curves of the extracts against *Acinetobacter baumannii* strains ATCC 17978 and AB5075 were plotted from data obtained from the broth microdilution MIC assay. Average and standard deviation of percent inhibition was calculated for each of the triplicates.

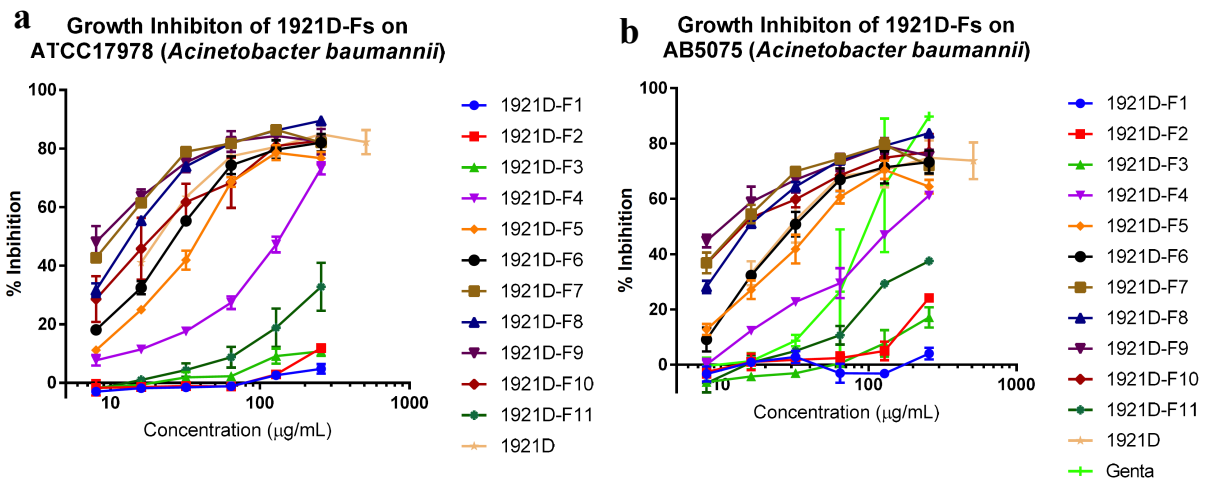

Figure 3.15. Percent growth inhibition of *Rosa* × *damascena* flash extracts against *Acinetobacter baumannii*. The x-axis is in log-10 scale. The error bar represents standard deviation within triplicate.

IC50 value was determined to be the concentration where 50% growth inhibition of the bacterium is achieved.

Table 3.2. IC50 of 1921D-F1~11 Against *Acinetobacter baumannii* (μg/mL)		
	ATCC 17978	AB5075
1921D-F1	--	--
1921D-F2	--	--
1921D-F3	--	--
1921D-F4	256	256
1921D-F5	64	64
1921D-F6	32	32
1921D-F7	16	16
1921D-F8	16	16
1921D-F9	16	16
1921D-F10	32	16
1921D-F11	--	--

4. TLC-agar-overlay bioautography assay

The normal-phase TLC plates of epigallocatechin gallate and 1921D-F7~9 were not treated with vanillin/sulfuric acid reagent and visualized under visible and UV light. For all three plates,

the Rf of epigallocatechin was about 0.6 and the banding patterns of the extracts were similar.

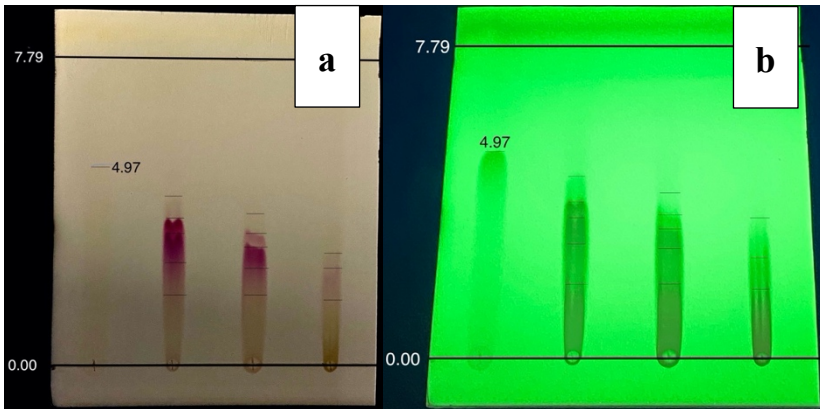

Figure 3.16. TLC plate 2 of epigallocatechin gallate and 1921D-F7~9 before TLC-agar-overlay bioautography assay. This is a picture of plate 2 under visible (a) and UV (b). The solvent front is 7.79 cm and the epigallocatechin ran to 4.97 cm. The streaks of extracts shown similar band pattern as before. The pattern was similar for plate 1 and 3.

After 22 hours of incubation, the LB soft agar turned from colorless, transparent and smooth to light blue with little bumps on top of the agar. The bumps of colonies were all over the agar, except for three regions of smooth surfaces directly on top of the streaks of extracts 1921D-F7~9. No zone of inhibition was observed on top of the streak of epigallocatechin gallate. The above phenomena could be observed in all three plates (Figure 3.17).

Table 3.3. Length of Inhibition Zone (cm) and Retention Factor (Rf) of 1921D-F7~9 in TLC-Agar Overlay Bioautography Assay Against AB5075

	1921D-F7		1921D-F8		1921D-F9	
	Length (cm)	Rf	Length (cm)	Rf	Length (cm)	Rf
Plate 1	2.0	0.24	2.0	0.24	1.9	0.22
Plate 2	3.0	0.39	2.9	0.37	2.2	0.28
Plate 3	2.8	0.36	2.8	0.36	2.0	0.26

For TLC plate 1, the lengths of inhibition zones for extracts 1921D-F7 and 1921D-F8 were shorter than those in plates 2 and 3; for plates 2 and 3, the lengths of clear zones were longer for extract 1921D-F7 and 1921D-F8 than that of 1921D-F9 (Table 3.3).

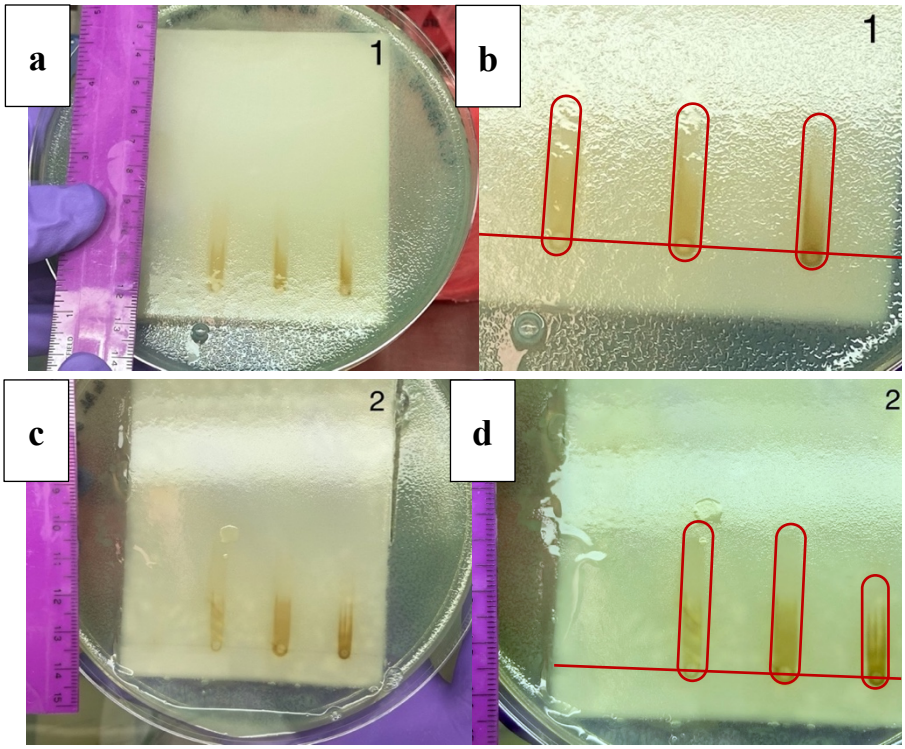

Figure 3.17. TLC plates of TLC-agar-overlay bioautography assay after 22-hour incubation. A. and b., plate 1; c. and d., plate 2. B. and d. are close-up image of the streak region; the clear regions in the agar were enclosed by the red shapes; the red lines were start line of the TLC run. Plates 1 and 2 were run under the same condition but not at the same time.

After another 22 hours of incubation, the blue color and the rough texture were more obvious on the plates. Some patches of colonies could be observed. Bumps of colonies started to grow on the streaks of extracts but the length of the smooth regions around the streaks of extracts 1921D-F7~9 generally remained unchanged.

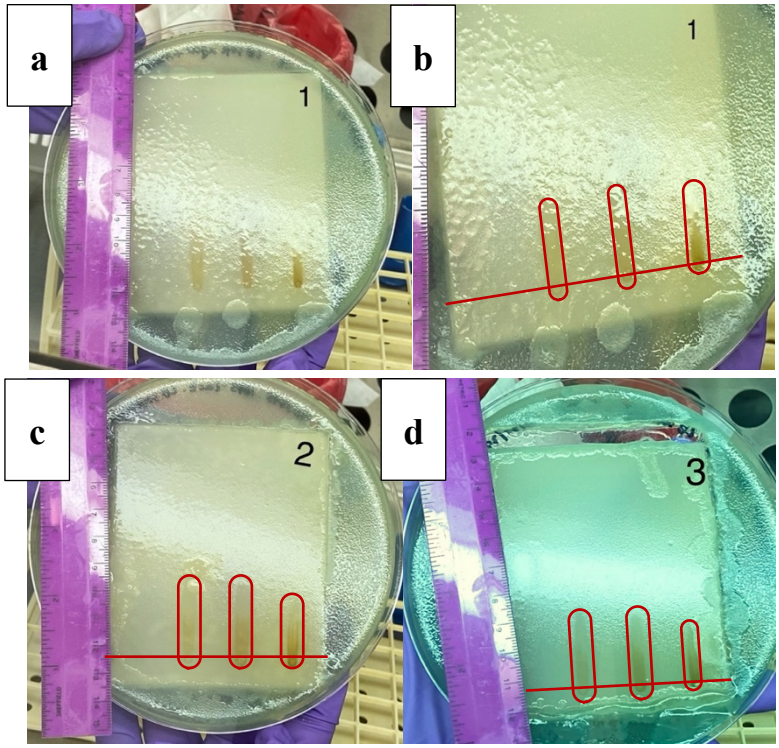

Figure 3.18. TLC plates of TLC-agar-overlay bioautography assay after 44-hour incubation. A. and b., plate 1; c. and d., plate 2. B. and d. are close-up image of the streak region; the clear regions in the agar were enclosed by the red shapes; the red lines were start line of the TLC run. TLC plates 1, 2 and 3 were run under the same condition, but plate 1 was not run at the same time as plates 2 and 3.

5. Reverse-phase TLC

After testing the different mobile phases, the optimal solvent system was determined to be chloroform:methanol:water (30:70:4, v/v/v). The trace of the extract stretched along the length of the solvent front. No obvious color pattern was observed under visible or UV light without the treatment of vanillin/sulfuric acid spraying reagent. The results for the other less optimal solvent system were not shown.

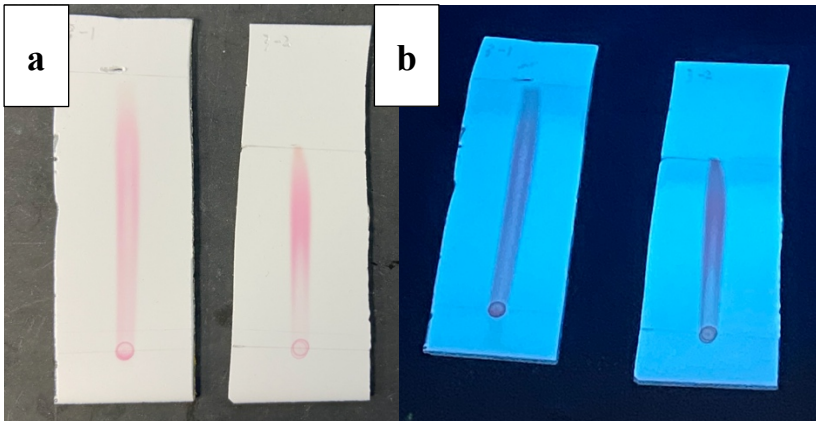

Figure 3.19. Reverse-phase TLC plates of 1921D-F7. The mobile phase was chloroform:methanol:water (30:70:4, v/v/v). The TLC plates were visualized under: a. visible light, b. UV light. The two plates were run under the same condition at different times.

6. Cytotoxicity test

The cytotoxicity curves of the active extracts 1921, 1921D and 1921D-F7~9 were plotted from data obtained from the broth microdilution MIC assay. Average and standard deviation of percent of inhibition was calculated for each triplicate.

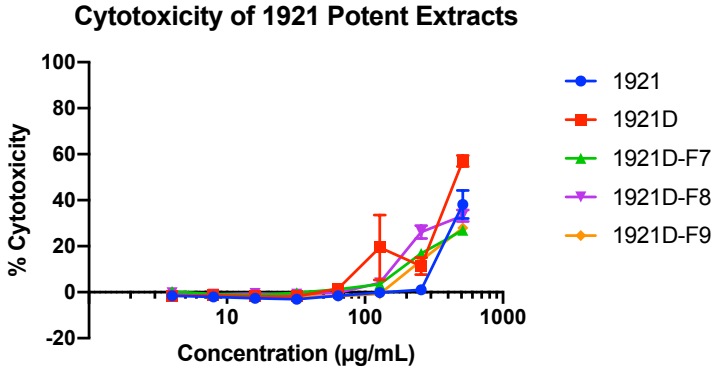

Figure 3.20. Percent cytotoxicity of potent extracts 1921, 1921D and 1921D-F7~9. The x-axis is in log-10 scale. The error bar represents standard deviation within each triplicate.

Chapter 4: Discussion

Overall fractionation scheme

As fractionation of *Rosa* × *damascena* flower proceeded from crude extract 1921to 1921D and to 1921D-F7~9, the IC50 concentration against both strains of *Acinetobacter baumannii*, ATCC 17978 and AB5075, continuously decreased. It can be conjectured that the concentration of the potent compound(s) increased as the number of different chemicals in each fraction decreased. Therefore, the bioassay-guided fractionation scheme was effective in approaching the goal of isolating effective components from the flower extract of *Rosa* × *damascena*.

Chemical properties of *Rosa* × *damascena* potent extracts

1. Analytical HPLC

For the reverse-phase analytical high-performance liquid chromatography (HPLC), the stationary phase used for separation is a nonpolar C18 column. Since the relative polarity of solvent (A) 0.1% formic acid in water, is higher than that of solvent (B) 0.1% formic acid in acetonitrile, as the concentration of solvent (B) increased through the run, the overall polarity of the mobile phase gradually decreased. Therefore, the more polar compounds in the extracts would elute earlier when the concentration of solvent (B) is lower, and the nonpolar compounds would elute later. However, the HPLC can only detect the presence of compounds that absorb the set wavelengths of UV light. For this reason, compounds that do not absorb UV light will not appear on the HPLC chromatogram, and the chromatogram might not represent the whole chemical profile of the extracts.

The chromatograms of the active extracts 1921D and 1921D-F7~9 consistently had most of their peaks eluting early in the run. The absorbance peaks of another active fraction 1921C also appeared when the mobile phase was more polar, while for fraction 1921B which didn't show much growth inhibitory activity, all of the peaks eluted with nonpolar mobile phase (Figure 3.2-6). The major peaks of 1921D and 1921D-F7~9 eluted when the concentration of solvent (B) was 5% to 25%. For these reasons, it is reasonable to suggest that the UV-active compounds and the bioactive compounds in the active extracts were very polar.

After comparison, the chromatogram of 1921D and its active flash fractions 1921D-F7~9 were found to be very similar (Figure 3.11-14), indicating that similar UV-active chemicals were present in the extracts.

2. Normal-phase Reverse-phase TLC

The solid phase used in the normal-phase thin-layer chromatography was a polar silica plate. The more polar compounds would stick more closely to the silica plate and move the least, which corresponds to an early eluting time in the HPLC chromatogram; nonpolar compounds would have the opposite characteristics. After being treated with vanillin/sulfuric acid spraying reagent, the potent extracts separated via TLC showed similar components near the start line and only varied near the solvent front (Figure 3.10). Therefore, it is confirmed that although the HPLC chromatograms of extracts 1921D and 1921D-F7~9 were similar, their chemical compositions were actually different. Since the growth inhibitory activities of 1921D-F7~9 were similar, it is conjectured that the shared, more polar compounds near the start line were responsible for the

antimicrobial activity. Each color on the streak on the TLC plate indicated the presence of at least one different compound: 1921D-F7 had at least four different compounds, while 1921D-F8 and 9 only had two (Figure 3.10). Since the distinct compound extracts 1921D-F7 were closer to the solvent front, the compounds that were missing in 1921D-F8 and 9 should be the more polar compounds.

For the reverse-phase TLC, the solid phase is nonpolar, and polar compounds tend to go closely with the mobile phase. After testing with the solvent systems (results not shown), the optimal mobile phase was chloroform:methanol:water (70:30:4, v/v/v). Extract 1921D-F7 stretched along the plate and stayed with the mobile phase. Therefore, the results from normal-phase and reverse-phase TLC agreed with that from reverse-phase HPLC, suggesting the compounds are polar.

Overall, the results from HPLC, normal-phase TLC and reverse-phase TLC agreed with each other. Therefore, the potent component(s) of *Rosa* × *damascena* flower extract is polar, which agrees with previous research that the phenolic compounds in the extract should be responsible for its antimicrobial activity.

Biological activity of *Rosa* × *damascena* potent extracts

1. Broth microdilution MIC assay of 1921 and 1921B~E against ESKAPE pathogens

In the broth microdilution MIC assay of extracts 1921 and 1921B~E against the ESKAPE pathogens, the extracts demonstrated up to 80% growth inhibitory activity at 512 g/mL against both strains of *Acinetobacter baumannii* (ATCC 17978, AB5075) and *Pseudomonas aeruginosa* (PAO1). The extracts also showed weak inhibition up to around 60% at 512 g/mL against

Enterobacter cloacae (CDC32), *Klebsiella pneumoniae* (EU32) and *Staphylococcus aureus* (AH1263). For the above bacteria, extracts 1921C and 1921D generally had the most inhibitory effect, followed by the crude extract 1921; 1921B and 1921E tended to have the least growth inhibition. The exception was in the treatment of *Enterococcus faecium* (EU49), where all extracts, except for 1921B, seemed to promote the growth of the bacterium, while 1921B could reach up to around 100% inhibition at high concentrations.

None of the extracts reached 90% growth inhibition, therefore no MIC value was obtained. The IC50 values of extracts 1921C and 1921D were the lowest, indicating that they had the strongest antimicrobial effect and likely captured the potent compound(s). Out of the two, 1921D was chosen to be further fractionated because it had better growth inhibitory activity against both strains of *A. baumannii* at low concentrations compared to 1921C. However, 1921C is a good direction for further elucidation.

2. Broth microdilution MIC assay of 1921D-Fs against *A. baumannii* strains

In broth microdilution MIC assay of the flash fractions of 1921D, extracts 1921D-F7~9 demonstrated the highest percentage of growth inhibition, followed by extracts 1921D-F5, 6, 10. Extracts 1921D-F1-4 and 11 had little inhibitory effect. The growth inhibition curves for the two strains of *A. baumannii* were very similar, yet the percent inhibition against the more virulent AB5075 strain was slightly lower than that for the susceptible ATCC 17978 strain. This indicated that the extract had lower inhibition against AB5075 probably due to the unique virulent or resistant factors within its genome.

However, although at 256 μg/mL extracts 1921D-F8 reached around 89% and 84% inhibition against ATCC 17978 and AB5075 respectively, none of the extracts reached 90% inhibition, and therefore no MIC value was obtained.

3. TLC-agar-overlay Bioautography assay

The *Acinetobacter baumannii* strain used in the assay was AB5075 modified with an insertion of Lac-Z gene. It is the production of ß-galactosidase encoded within the Lac operon, which is responsible for the digestion of lactose in many enteric bacteria. The added X-gal in the LB soft agar used to culture the modified bacteria is an analog of lactose. The colorless compound is made up of a galactose and an indole, which upon hydrolysis by ß-galactosidase will yield a blue product. For this reason, the growth of AB5075 can be indicated by the color change from colorless to blue or by visible colonies in the agar.

For the three TLC plates tested in the assay, the development of a rough surface with little bumps indicated the presence of bacterial colonies. The color was changed to slightly blue. The clear zones on and slightly around the streaks of extracts indicated that there was growth inhibition against the bacterium. The length of the zone of inhibition was similar for extracts 1921D-F7~9 in plate 1, but the length for 1921D-F7 and 8 was longer than that of 1921D-F9 in plates 2 and 3. Since TLC plate 1 was not run at the same time as TLC plates 2 and 3, variation could arise. By comparing the Rf values of the zones of inhibition in plate 2 to the image of plate 2 taken before the assay, the zone of inhibition was found to cover the majority the streaks. This indicated that for extracts 1921D-F7~9, the majority of the fractions had growth inhibitory activity against *A.*

baumannii. It could that most of the compounds in the extracts were potent, or that separation of the fractions was not enough. Therefore, it is reasonable to suggest that fractionation using flash chromatography was not optimal for this extract and further separation is needed.

4. Cytotoxicity test

The highest percent cytotoxicity for the active extracts was around 30-40%. The extract 1921 had the least cytotoxicity while cytotoxicity was highest for extract 1921D. Among the three flash fractions, 1921D-F9 had the lowest cytotoxicity that is closest to the level of 1921 (Figure 3.20.). The cytotoxicity of the extract could increase because the concentration of certain compound(s) in the extract increased as fraction proceeded. However, the cytotoxicity for the extracts was generally low, which went down to around 0% starting at 128 μg/mL.

Conclusion

The *Rosa* × *damascena* flower extract had growth inhibitory effect against *Acinetobacter baumannii*. In broth microdilution assay, potent extracts 1921D-F7~9 demonstrated similar growth inhibitory activity with IC50 at 32 μg/mL; 90% inhibition wasn't reached. Extracts 1921D-F7~9 shared similar chemical composition and the active compound(s) is likely polar. The active extracts had low cytotoxicity to human cells.

Future Direction

Since the active extracts and the compounds are likely polar, flash chromatography will not be able to reach optimal fractionation. Since the chromatogram of analytical HPLC showed clear

separation of peaks, preparative HPLC might be utilized to further fractionate the potent extracts 1921D-F7~9 more definitively.

Further optimization of the reverse-phase TLC method can be done. If better separation is reached, TLC-agar-overlay assay could again be used to elucidate which fraction of 1921D-F7~9 contain the active compound(s).

References Cited

1. Lee CR, Lee JH, Park M, Park KS, Bae IK, Kim YB, et al. Biology of Acinetobacter baumannii: Pathogenesis, Antibiotic Resistance Mechanisms, and Prospective Treatment Options. Frontiers in Cellular and Infection Microbiology. 2017;7:35. doi: 10.3389/fcimb.2017.00055. PubMed PMID: WOS:000396176600001.
2. Antunes LCS, Visca P, Towner KJ. Acinetobacter baumannii: evolution of a global pathogen. Pathogens and Disease. 2014;71(3):292-301. doi: 10.1111/2049-632x.12125. PubMed PMID: BIOSIS:PREV201400644534.
3. Harding CM, Hennon SW, Feldman MF. Uncovering the mechanisms of Acinetobacter baumannii virulence. Nature Reviews Microbiology. 2018;16(2):91-102. doi: 10.1038/nrmicro.2017.148. PubMed PMID: BIOSIS:PREV201800212512.
4. Wong D, Nielsen TB, Bonomo RA, Pantapalangkoor P, Luna B, Spellberg B. Clinical and Pathophysiological Overview of Acinetobacter Infections: a Century of Challenges. Clin Microbiol Rev. 2017;30(1):409-47. doi: 10.1128/cmr.00058-16. PubMed PMID: BIOSIS:PREV201700277844.
5. Higgins PG, Dammhayn C, Hackel M, Seifert H. Global spread of carbapenem-resistant Acinetobacter baumannii. Journal of Antimicrobial Chemotherapy. 2010;65(2):233-8. doi: 10.1093/jac/dkp428. PubMed PMID: BIOSIS:PREV201000118667.
6. Otter JA, Yezli S, French GL. The Role Played by Contaminated Surfaces in the Transmission of Nosocomial Pathogens. Infection Control and Hospital Epidemiology. 2011;32(7):687-99. doi: 10.1086/660363. PubMed PMID: BIOSIS:PREV201100518119.
7. Aydemir H, Akduman D, Piskin N, Comert F, Horuz E, Terzi A, et al. Colistin vs. the combination of colistin and rifampicin for the treatment of carbapenem-resistant Acinetobacter baumannii ventilator-associated pneumonia. Epidemiology and Infection. 2013;141(6):1214-22. doi: 10.1017/s095026881200194x. PubMed PMID: BIOSIS:PREV201300418821.
8. Cai Y, Chai D, Wang R, Liang BB, Bai N. Colistin resistance of Acinetobacter baumannii: clinical reports, mechanisms and antimicrobial strategies. J Antimicrob Chemother. 2012;67(7):1607-15. doi: 10.1093/jac/dks084. PubMed PMID: WOS:000305086600005.
9. Jacobs AC, Thompson MG, Black CC, Kessler JL, Clark LP, McQueary CN, et al. AB5075, a Highly Virulent Isolate of Acinetobacter baumannii, as a Model Strain for the Evaluation of Pathogenesis and Antimicrobial Treatments. mBio. 2014;5(3):e01076-14. doi: 10.1128/mBio.01076-14. PubMed PMID: BIOSIS:PREV201400585117.
10. Ulusoy S, Bosgelmez-Tinaz G, Secilmis-Canbay H. Tocopherol, Carotene, Phenolic Contents and Antibacterial Properties of Rose Essential Oil, Hydrosol and Absolute. Current Microbiology. 2009;59(5):554-8. doi: 10.1007/s00284-009-9475-y. PubMed PMID: BIOSIS:PREV200900617839.
11. Aridogan BC, Baydar H, Kaya S, Demirci M, Ozbasar D, Mumcu E. Antimicrobial activity and chemical composition of some essential oils. Archives of Pharmacal Research. 2002;25(6):860-4. PubMed PMID: WOS:000180186000019.
12. Boskabady MH, Shafei MN, Saberi Z, Amini S. Pharmacological Effects of Rosa

Damascena. Iranian Journal of Basic Medical Sciences. 2011;14(4):295-307. PubMed PMID: BIOSIS:PREV201100541933.
13. Pires TCSP, Dias MI, Barros L, Calhelha RC, Alves MJ, Oliveira MBPP, et al. Edible flowers as sources of phenolic compounds with bioactive potential. Food Research International. 2018;105:580-8. doi: 10.1016/j.foodres.2017.11.014. PubMed PMID: BIOSIS:PREV201800313827.
14. El Beyrouthy M, Arnold N, Delelis-Dusollier A, Dupont F. Plants used as remedies antirheumatic and antineuralgic in the traditional medicine of Lebanon. J Ethnopharmacol. 2008;120(3):315-34. Epub 2008/09/24. doi: 10.1016/j.jep.2008.08.024. PubMed PMID: 18809483.
15. Basim E, Basim H. Antibacterial activity of Rosa damascena essential oil. Fitoterapia. 2003;74(4):394-6. PubMed PMID: BIOSIS:PREV200300425411.
16. Ozkan G, Sagdic O, Baydar NG, Baydar H. Note: Antioxidant and antibacterial activities of Rosa damascena flower extracts. Food Science and Technology International. 2004;10(4):277-81. doi: 10.1177/1082013204045882. PubMed PMID: BIOSIS:PREV200400417675.
17. Adwan G, Abu-Shanab B, Adwan K. Antibacterial activities of some plant extracts alone and in combination with different antimicrobials against multidrug-resistant Pseudomonas aeruginosa strains. Asian Pac J Trop Med. 2010;3(4):266-. doi: 10.1016/s1995-7645(10)60064-8. PubMed PMID: WOS:000282853300004.
18. Reich E, Schibli A. High-performance thin-layer chromatography for the analysis of medicinal plants. New York: Thieme; 2007. xv, 264 p. p.